Recent Advances in Modeling and Experiments of Kevlar Ballistic Fibrils, Fibers, Yarns and Flexible Woven Textile Fabrics – A Review

Subramani Sockalingam[a,b], Sanjib C. Chowdhury[a], John W. Gillespie Jr[a,b,c,d] and Michael Keefe[a,b]

[a] *Center for Composite Materials, University of Delaware, DE, USA*
[b] *Department of Mechanical Engineering, University of Delaware, DE, USA*
[c] *Department of Materials Science and Engineering, University of Delaware, DE, USA*
[d] *Department of Civil and Environmental Engineering, University of Delaware, DE, USA*

Corresponding author:
Subramani Sockalingam, Center for Composite Materials, University of Delaware, Newark, DE 19716, USA
Email: sockalsi@udel.edu

Abstract

Ballistic impact onto flexible woven textile fabrics is a complicated multi-scale problem given the structural hierarchy of the materials, anisotropic material behavior, projectile geometry-fabric interactions, impact velocity and boundary conditions. Although this subject has been an active area of research for decades, the fundamental mechanisms such as material failure, dynamic response, multi-axial loading occurring at the lower length scales during impact are not well understood. This paper reviews the recent advances in modeling and experiments of Kevlar ballistic fibrils, fibers, yarns and flexible woven textile fabrics pertinent to the deformation modes occurring during impact and serves to identify topics worthy of further investigation that will advance the basic understanding of the phenomena governing transverse impact. This review also explores on aspects such as homogeneous versus heterogeneous behavior of yarns consisting of individual fibers and the inelastic transverse behavior of the fiber which is not considered in the previous review papers on this topic.

Keywords

Ballistic fiber, ballistic impact, finite element analysis (FEA), wave propagation

Introduction

High performance aramid (Kevlar®, Twaron®) and polyethylene (Spectra®, Dyneema®) fibers are widely used in ballistic impact applications such as soft body armor [1, 2] and gas turbine engine containment system [3] in the form of flexible textile fabrics. The textile fabrics are also used as a backing material in an armor system with a ceramic strike face. A generic fabric armor system subjected to impact and some of the physically observed mechanisms and deformation modes in the fabric are shown in Figure 1. Impact velocities lower than the wave speed of the material are the typical range for armor backings. Hence shock wave effects are not considered in this review. The impact response is often dependent on the projectile geometry, impact velocity, material behavior and boundary conditions. Generally speaking, the fabric layers closer to the impact site are subjected to local transverse compression and shear and the layers in the rear are loaded in in-plane tension.

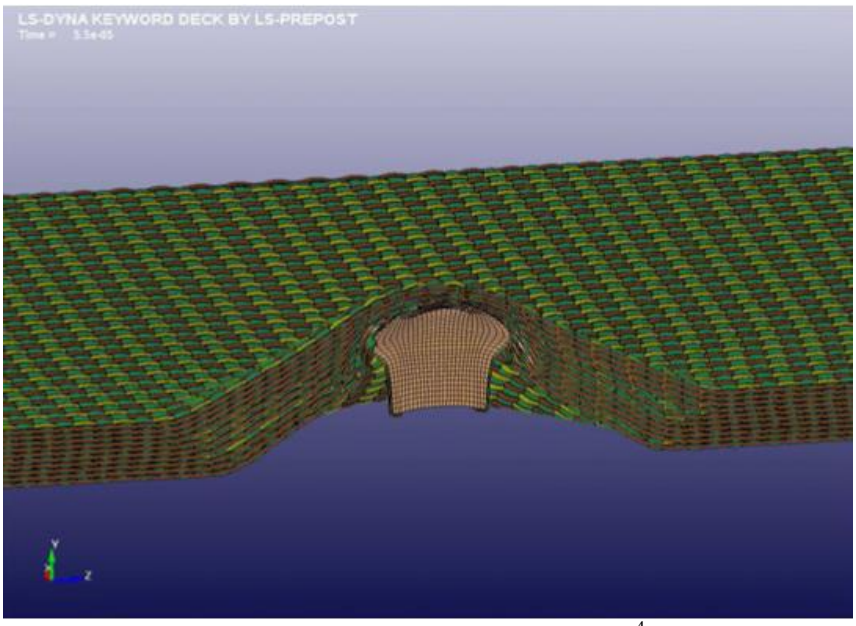

(a) Multiple fabric layers impacted (figure courtesy Chocron et al. [4])

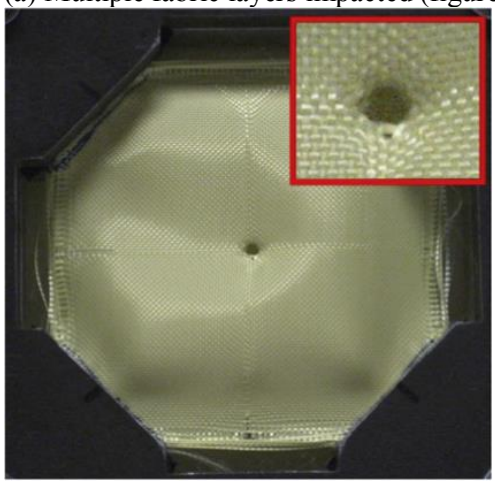

(b) Yarn pull out from fabric edges during ballistic impact testing (figure courtesy Nilakantan et al. [5])

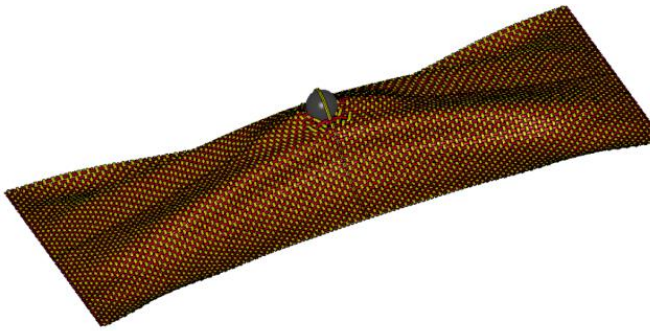

(c)Yarn pull out from fabric edges predicted by homogenized yarn model (figure courtesy Nilakantan et al. [6])

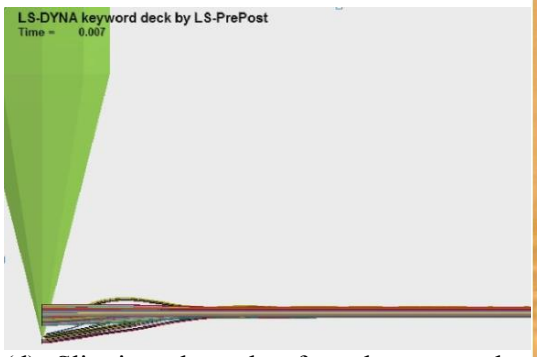

(d) Slipping through of a sharp nosed projectile

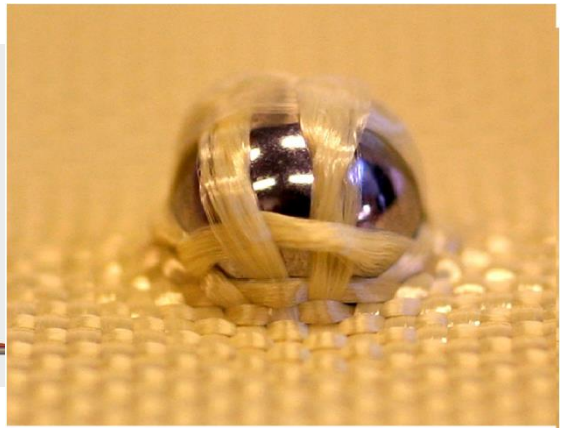

(e) Spherical projectile caught by the fabric (figure courtesy Nilakantan et al. [5])

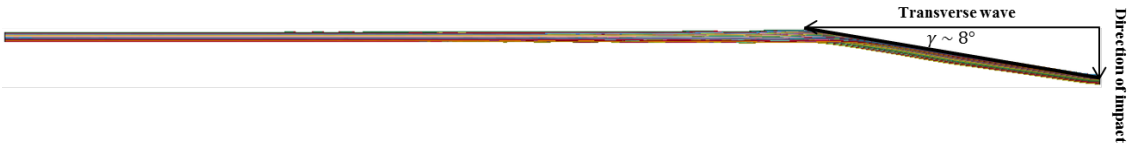

(f) Longitudinal and transverse wave propagation in a yarn, transverse compression and shear

(g) Fiber-fiber interactions – spreading and flattening of fibers within a yarn [7]

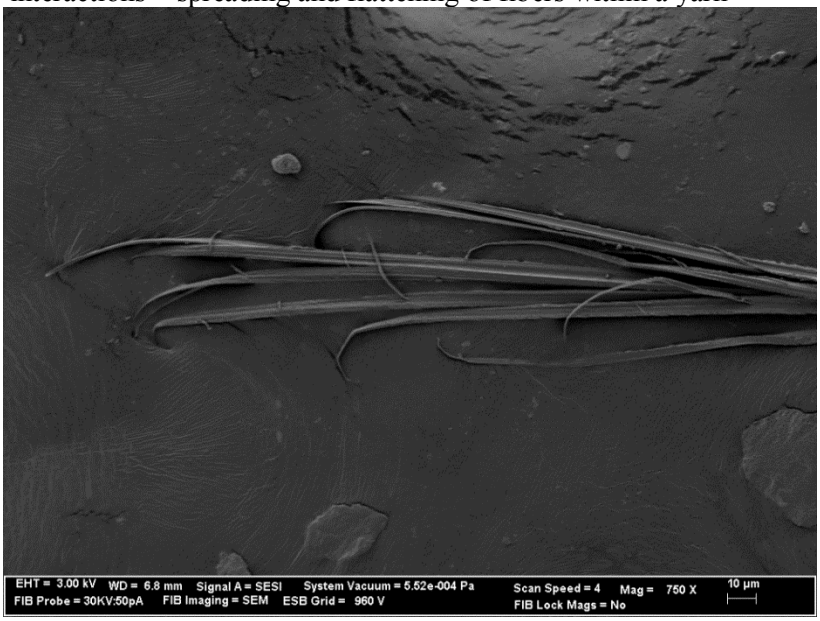

(h) Fibrillated failure of Kevlar KM2 single fiber

Figure 1. Mechanisms, deformation and failure modes in a generic fabric armor at multiple length scales

The textile fabrics possess a hierarchical multi-scale architecture from fibrils to fibers to yarns (tows) to multi-layer fabrics as shown in Figure 2(a). Kevlar (p-phenylene terephthalamide, PPTA) is an aromatic polyamide (i.e., aramid) type polymeric material. In the aromatic structure of Kevlar chain, adjacent phenylene rings are connected through amide group (see Figure 2) while the phenylene rings stay preferably in trans-stereo-isomeric conformation. The foundational element of Kevlar fiber is the crystalline lattice. Figure 2(b) and (c) shows the orthorhombic PPTA crystal structure proposed by Northolt et al. [8, 9] and Tashiro et al. [10]. This unit cell contains two molecular repeating units per crystal lattice, one at the center of the cell and four one-fourth at each corner of the cell. In the bc lattice plane, hydrogen bonds are formed between the neighboring NH and CO end groups due to the close proximity of the chains. While in the ab plane, there is no hydrogen bonding between the chains, the only interactions are non-bonded van der Waals (vdW) and coulombic. In terms of bonding strength, vdW and coulombic

interaction are weaker than hydrogen bond and hydrogen bonds are weaker than covalent bond existing between different atoms in the chain. Therefore, from a mechanics perspective, the crystal is anisotropic and is stronger in the *c* axis, weaker in the *b* axis and weakest in the *a* axis. In the hierarchical scale, the crystals evolve into macromolecules/fibril and the fibrils evolve into filament/fiber. Therefore the fiber properties are superior in the oriented fiber direction compared to the transverse direction. Kevlar fibers have a thermal decomposition temperature of ~ 500 ^{o}C [11] due to the high stability of aromatic structures.

Polyethylene fibers are made up of extremely long chains of polyethylene (monomer unit > 250,000 per molecule). The chains become highly oriented along the fiber axis during the deformation process induced by shear, compression or tension. At the crystal level, polyethylene exhibits three types of unit cell – orthorhombic, monoclinic, and hexagonal [12-15].The orthorhombic unit cell is by far the most common. Each orthorhombic unit cell contains a complete ethylene unit from one chain segment and part of four others from surrounding chain segments, for a total of two per unit cell. The precise morphology of fibers is a function of many factors, including the structure prior to deformation and the process by which orientation was achieved. The molecular alignment developed during orientation strongly influences the properties of the resulting products; higher levels of orientation magnify the anisotropic response to external forces. Unlike Kevlar, the melting temperature of polyethylene is low (~145 ^{o}C) [16]. Prevorsek et al. [16] reported that the projectile fiber frictional interactions result in an increase in temperature at the projectile/armor interface above the melting point of high performance polyethylene fiber. However they noted due to the short time scale during ballistic impact, the temperature is rise limited to a very small region and its effects on the armor performance cannot be detected. Predicting the mechanical and impact response of these materials and thus designing the protective/containment system is a challenge. The impact experiments on yarns and fabrics are not only expensive but also complicated due to the fiber-fiber and yarn-yarn interactions. Therefore a combined numerical modeling and experimental approach is typically adopted to understand the system response. With advances in experimental techniques and computational power, some of the recent researches have focused on understanding the fundamental mechanisms during impact particularly at lower length scales.

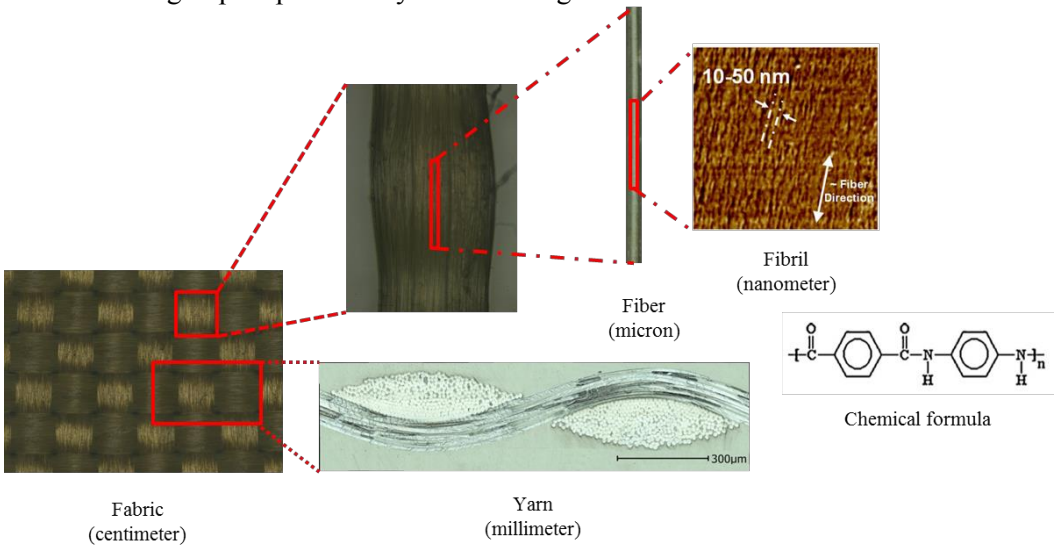

(a)

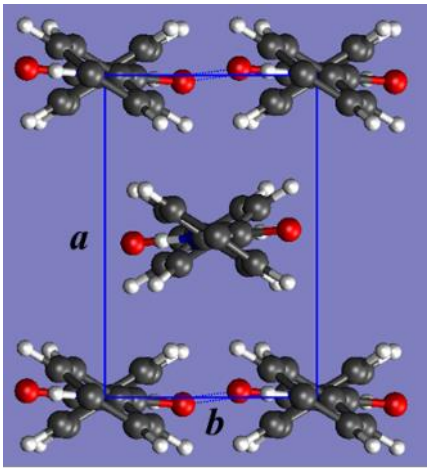

(b)

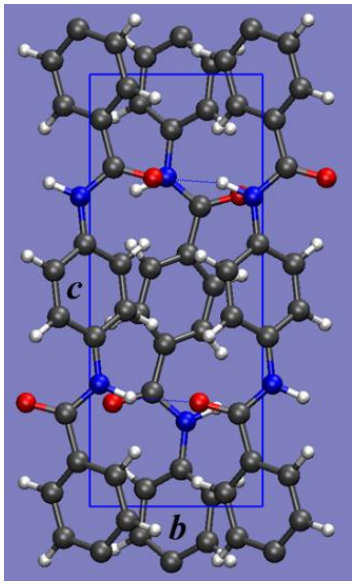

(c)

Figure 2. (a) Multi-scale architecture of Kevlar K706 fabric with KM2 fibers (b) Kevlar crystal lattice [8-10] (b) ab plane view (c) bc plane view Atom color : gray – carbon, white – hydrogen, red – oxygen, blue – nitrogen

The review papers published on this topic include the works by Cheeseman and Bogetti [17], Tabiei and Nilakantan [18] and David et al. [19]. These review papers introduce the key factors that influence the ballistic performance of fabrics from a multi-scale perspective such that the fabrics comprised of woven yarns can be modeled as a homogeneous orthotropic elastic material and that tensile properties in the yarn direction govern dynamic response during impact. There is limited review on the responsible mechanisms associated with different length scales where yarns are considered as heterogeneous (e.g. KM2 600 denier yarn has 400 hundred individual fibers), fibers within an impacted yarn are loaded non-uniformly, subjected to multi-axial loading and failure is governed by the inelastic transverse behavior of the fiber. The goal of this paper is to review the recent research in modeling and experiments of important mechanisms and deformation modes of these materials (primarily focused on plain woven aramid fabrics) at different length scales. The theory of transverse impact is first reviewed. Then the impact experiments and mechanical characterization experiments at different length scales relevant to the deformation modes experienced by the material during impact are discussed. Finally modeling of ballistic fibrils to multi-layer fabrics is reviewed. The authors recognize the complexity of penetration mechanics of armor [20], which will not be considered in detail here.

Theory of Transverse Impact

Transverse impact: classical Smith theory

The theory of transverse impact onto a homogenous yarn shown in Figure 3 was developed by Smith et al. [21, 22]. The transverse impact initiates a longitudinal strain wave that propagates at a speed given by $\mathbf{c} = \sqrt{\frac{\mathbf{E}}{\boldsymbol{\rho}}}$ and a transverse wave ('V' shaped) that propagates with a speed an order of magnitude lower than the longitudinal wave. The angle made by the transverse wave (Lagrangian transverse speed U) with the horizontal is a constant for the region $\mathbf{0} \leq \mathbf{x} \leq \mathbf{Ut}$. That

is the transverse wave is a straight line assuming tension as the only restoring force in the fiber for this analytical solution.
It is noted that 1D analytical solution for transverse impact onto a fiber or a homogenous yarn [21, 23] assumes linear elastic small strains with tension in the fiber as the only restoring force and long fibers (to avoid complications of wave reflections). The boundary condition is constant velocity (V) impact at a point. Therefore they do not consider the effect of projectile geometry, interlaminar shear (in the plane of fiber direction-impact direction) or the wave propagation through the thickness of the fibers that are loaded in compression directly under the impactor.

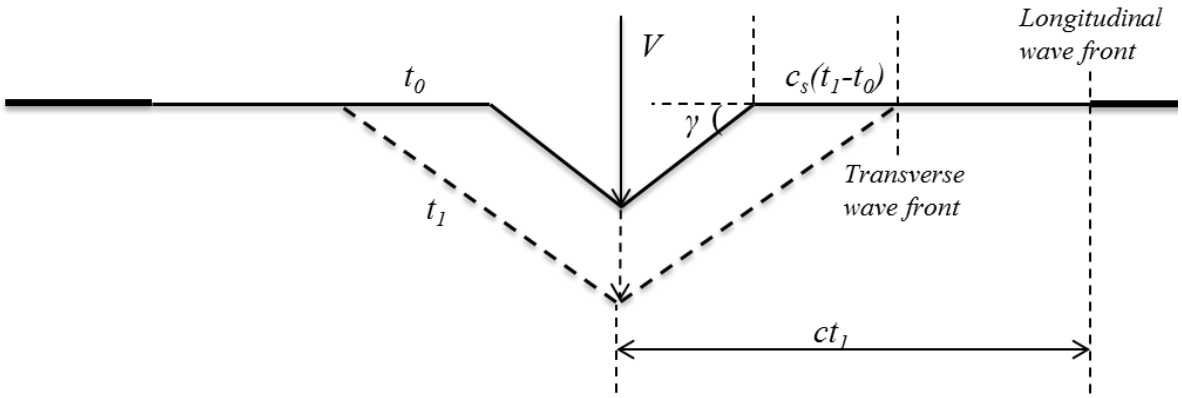

Figure 3. Transverse impact

The strain (implicitly) in the fiber behind the longitudinal wave and the Euler transverse wave speed are given by Equations 1 and 2

$$V = c\sqrt{2\varepsilon\sqrt{\varepsilon(1+\varepsilon)} - \varepsilon^2} \tag{1}$$

$$u_{lab} = c\left(\sqrt{\varepsilon(1+\varepsilon)} - \varepsilon\right) \tag{2}$$

where ε is the strain in the fiber and V is the impact velocity. The transverse wave speed increases when it interacts with a reflected longitudinal wave [22]. Alternately the transverse wave speed c_s derived by Cole et al. [24] and Wang [25] for the case $c_s \ll c$ is given by

$$c_s = \left(\frac{c}{2}\right)^{1/3} (V)^{2/3} \tag{3}$$

The 'V' angle γ made by the transverse wave with the horizontal direction as shown in Figure 3 is given by Equation 4 [26].

$$\gamma = \tan^{-1}\left(\frac{2V}{c}\right)^{1/3} \tag{4}$$

Classical theory (Equation 1) predicts an impact velocity of 849 m/s to break the fiber for a failure strain of 3.55% for Kevlar KM2 fiber [1]. It should be noted that breaking speed is defined as the speed at which the fiber/yarn fails immediately upon contact with the projectile. Although experimental breaking speed for single fibers are not reported in the literature to our knowledge, breaking speeds for yarns (KM2, Dyneema® SK-65 and PBO®) reported in Walker and Chocron [27] is up to 40% lower than the classical breaking speed.

Transverse impact: modified theory

Walker and Chocron [27] extended the classical Smith theory to account for large strains using the first Piola-Kirchhoff stress measure in the undeformed configuration. For small strain case their solution is given by

$$V = c(E_{11})^{3/4}\sqrt{2-\sqrt{E_{11}}} \quad (5)$$

where E_{11} is the axial component of the Green strain. This extension still assumes axial tensile modulus and density are the only properties affecting the solution. The experimental observations of lower breaking speed for yarns compared to the classical theoretical speed is explained as due to the waves from the edges of the flat faced projectile that interacts at the center of the yarn. Also homogenized yarn computational models showed bounce of the yarn in front of the projectile [4, 28] due to elastic collision. Therefore a relationship is derived between the impact velocity, bounce velocity and strain in the material for a flat faced projectile [27]. When the bounce velocity is equal to the impact velocity, the breaking speed is predicted to be 11% less than the classical breaking speed. However when the bounce velocity is twice the impact velocity (upper bound for an elastic collision) the breaking speed is predicted to be lowered up to 40% due to the increase in the axial strain. It should be noted that bouncing of the yarn (in KM2 and Dyneema®) is not observed experimentally. This study clearly shows that the interactions between the impactor and fibers are important factors governing failure of the fiber as well as the experimental set-up required for accurate characterization.

It should be noted that classical theory and modified theory do not differentiate between a single fiber and a yarn as they consider only axial tensile loads and the longitudinal wave speed. As will be discussed later, the transverse impact of a yarn consisting of many interacting fibers is very different. Although 1D solution provides an understanding of wave propagation during impact, a more thorough model is needed to understand the fabric system response. Phoenix and Porwal [29, 30] developed an analytical solution for a 2D isotropic membrane impacted by a cylindrical projectile. Their solution provided good agreement with the multi-ply fabric experimental data of Cunniff [31] and closely followed Cunniff's empirical curves. However, a fabric based membrane is orthotropic and idealizing fabric architecture as a membrane does not allow the lower length scale energy absorbing mechanisms to be modeled accurately (e.g. yarn compression, yarn pull-out, windowing and friction between yarns and impactor, etc.).

Cunniff equation

Cunniff [31] empirically related the ballistic performance of the armor system (both fabrics and composites of different areal densities) to the fiber mechanical properties, specifically the product of fiber specific toughness and acoustic wave speed given by

$$\Phi\left(\frac{V_{50}}{(U^*)^{1/3}}, \frac{A_d A_p}{m_p}\right) = 0 \quad (6)$$

$$(U^*)^{1/3} = \left(\frac{\sigma_f \varepsilon_f}{2\rho_f}\sqrt{\frac{E_f}{\rho_f}}\right)^{1/3} \quad (7)$$

where V_{50} is the ballistic limit, A_d is the areal density, A_p is the projectile presented area, m_p is the projectile mass, σ_f is the fiber tensile failure strength, ε_f is the fiber tensile failure strain, ρ_f is the fiber density and E_f is the fiber tensile modulus assuming the fiber behavior is linear elastic. He plotted V_{50} against the dimensionless parameter that relate the projectile characteristics to the armor configuration $\frac{A_d A_p}{m_p}$ and showed good correlation with Equation 7 for different armor systems except ultra high molecular weight polyethylene (UHMWPE) Spectra. It is argued that this deviation may be due to the lower melting point of the thermoplastic Spectra fibers [1]. These models also assume transverse compression of the fibers do not contribute to energy absorption or

degrade the fiber tensile strength and do not account for the statistical nature of fiber failure. Table 1 shows the Cunniff velocity (Equation 7) and theoretical breaking speed (Equation 1) for some common ballistic fibers with properties from [1]. It is seen that the theoretical breaking speed is much higher than the Cunniff velocity. While Smith's equation 1 depends on the wave speed and failure strain, Cuniff's equation depends on the wave speed and the fiber specific toughness and thus more realistic.

The relationship between the yarn mechanical properties to the ballistic performance of a multi-layer fabric is complex [32] and it is important to consider the compressive properties, temperature, fiber-fiber friction and layer-layer interactions. Based on V_{50} (defined in the next section below) testing, Cunniff's equation is found to be in agreement for Kevlar fibers with low failure strain (3.6 to 4.4%) which showed fibrillated failure [32]. However Cunniff's equation is not in agreement for experimental poly (ethylene naphthalate) (PEN) fibers with high failure strain (8 to 18%) which showed melting [32] and UHMWPE composites [33] which showed a shear strength dependent ballistic limit. It should be noted that melting and shear was not a mechanism considered by Cunniff.

Table 1. Cunniff velocity and theoretical breaking speed for common ballistic fibers

Fiber	**Density (g/cm^3)**	**Modulus (GPa)**	**Failure strain (%)**	**Cunniff velocity (m/s)**	**Theoretical breaking speed (m/s)**
Spectra 1000	0.97	120	3.50	801	1223
Dyneema SK76	0.97	116	3.50	892	1202
Kevlar KM2	1.44	82.6	3.55	682	849
Carbon fiber	1.80	227	1.76	593	744
E-glass fiber	2.89	74	4.70	559	690

While the analytical models provide useful insights and indicate the relative ballistic performance of fibers, they do not account for many other contributing factors including compressive properties, interlaminar shear, strain rate effects, fiber-specific failure modes, projectile-fiber interactions, effect of projectile geometry, fiber-fiber and yarn-yarn interactions, 3D stress states, multi-axial loadings and so on. To understand these effects, one must consider modeling and experiments of these deformation mechanisms at the appropriate length scales.

Experiments on Fibrils, Fibers, Yarns and Fabrics

At the fabric macro length scale, National Institute of Justice NIJ standard 0101.06 [34] provides minimum performance requirements and test methods for the ballistic resistance of body armor. V_{50} ballistic limit is one of the widely used measures of characterizing the ballistic performance of the armor system and is defined as the velocity at which the projectile is expected to perforate the armor 50% of the time. V_{50} ballistic limit is determined through an experimental statistical evaluation of the armor system without consideration of material response at lower length scales. Consequently due to the complexity of ballistic impact onto flexible materials involving multiple layers and length scales, experiments conducted at lower length scales can isolate the underlying mechanisms and provide a better understanding. These experiments can then be used to validate the numerical models at the same length scales. This section reviews some of the ballistic impact experiments on fabrics and mechanical characterization experiments on these materials at different length scales and strain rates.

Fabric length scale experiments

The textile fabrics can be woven from yarns in many different styles. Dong and Sun [35] list five different styles of plain woven Kevlar fabrics using different Kevlar fibers with their axial

modulus. For example, Kevlar K706 fabric consists of KM2 fibers, 600 denier yarns, and 34 yarns per inch in warp and weft directions. The K706 fabric has a thickness of 0.23 mm and a span of 0.747 mm. Traditionally, ballistic impact experiments on the fabric systems focused on the relationship between the impact velocity and residual velocity for a given projectile and determining the V_{50} ballistic limit. However some of the recent work looked at understanding the wave propagation, failure mechanisms related to projectile geometry and progressive fiber failure as discussed below.

A qualitative description of the fabric impact mechanics is provided by Cunniff [36]. Longitudinal and transverse waves develop and propagate in the yarns in a fabric that are in direct contact with the projectile during impact. The longitudinal waves in the primary yarns drive the longitudinal waves in the secondary yarns as shown in Figure 4 thus providing an effective transverse impact on the secondary yarns. The secondary yarns constrain the motion of the primary yarns resulting in tensile strain gradient as observed by the significant curvature during transverse deflection of a single ply fabric. The longitudinal wave speed in a fabric is approximately $c_{\text{fabric}} = \frac{c_{\text{yarn}}}{\sqrt{2}}$ [37]. A similar explanation is provided by Chocron et al. [37, 38] based on their measured strains in the secondary yarns consistent with Cunniff's description. They measured strains in a multi-layer Kevlar fabric during ballistic impact by embedding Nickel-Chromium (NiCr) wires in the secondary yarns. NiCr high resistivity wire has the property to change its resistance (and voltage) due to applied strains. The pyramid transverse wave propagation during the impact of a flexible fabric is experimentally observed for both traditional fabrics [28] and unidirectional fibers held together by a polyurethane matrix (Dyneema® HB80) [39]. The transverse wave speed, unlike longitudinal wave speed depends on both material properties (longitudinal wave speed) and loading conditions (impact velocity) and is confirmed by these experiments. The wave propagation information can thus be used to validate the fabric properties of a fabric length scale model.

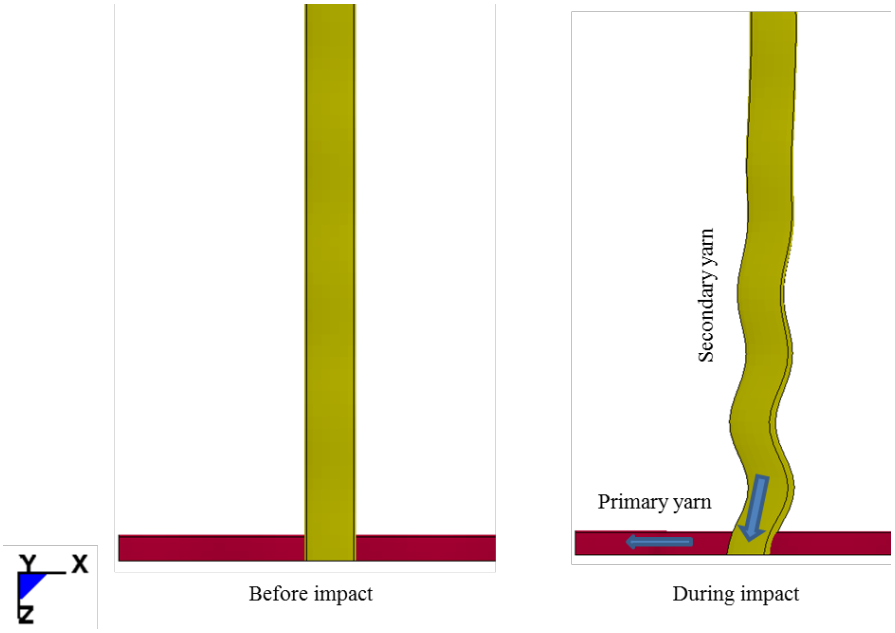

(a)

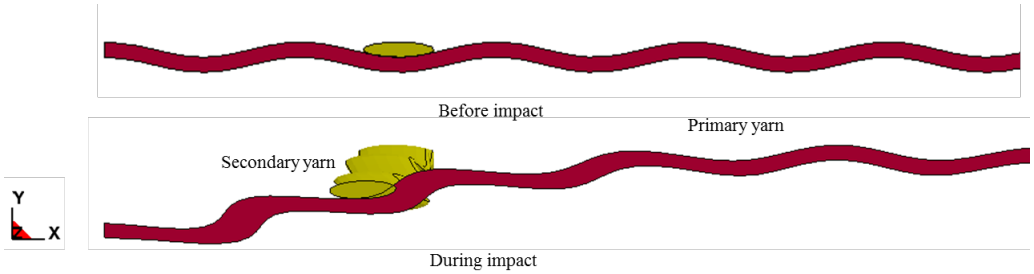

(b)

Figure 4. Fabric (plain woven) impact mechanics (a) top view (b) side view (displacement exaggerated)

The projectile geometry not only affects the ballistic limit but also plays a major role on the energy absorption behavior and failure mechanisms [40-43]. Yarn pullout is reported most for hemispherical and least for ogival and conical projectiles as they can slip through the fibers due to their sharp nose as shown in Figure 1(d). Fibrillation is a predominant failure mechanism for sharp nosed projectiles where splitting of fiber occurs along and perpendicular to their length. This fibrillation is attributed to the breaking of secondary hydrogen bonds in aramid fibers [40]. Frictional mechanisms including fiber breakage at the yarn crossovers, flattening and rupture of fibers, yarn pull out are also physically observed [40]. Severe flattening of fibers is observed for a hemispherical and flat headed projectile impact [40]. Significant transverse permanent deformation of the fibers is observed from post failure investigation of impacted fabrics [44, 45]. In a multi-layer plain woven fabric system, the first few layers are subjected to transverse shear and compression [36]. While the fibers in the front layer closer to the impact site are found to fail in shear failure mode due to the edge of a cylindrical flat ended projectile, fibers in the rear layer display fibrillation due to tensile failure [46]. Projectile obliquity is also found to influence the ballistic limit [47]. These experimental observations on projectile geometry dependent failure mechanisms are critical in setting up lower length scale experiments to better understand these interactions. Several researchers report the influence of boundary conditions on the impact response of fabric systems [36, 48, 49] and also note slippage of fabric from clamped edges [49, 50]. In general, slippage leads to decrease in primary yarn tension resulting in higher energy absorption than without slippage. Parsons et al. [50] report the usage of knurled clamps to minimize slipping of the fabric. The nature and manufacturing of the textile fabrics and armor system allows infinite possibilities of configurations to achieve optimum ballistic performance through a materials-by-design approach. The fabric weave type [51, 52], weave density [53], number of filaments [54] and hybrid fabric panels [55] are some of the design variables which affects the ballistic performance.

To gain more insight into the fabric deformation behavior researchers conducted mechanical characterization experiments including quasi static (QS) and dynamic tension, in-plane shear and transverse compression tests. A bilinear load displacement uniaxial response – a low modulus decrimping region followed by a high modulus elongation regime is observed for silica nanoparticle impregnated fabrics [56]. The deformation in a fabric is governed by yarn interactions at the cross over points. While the yarns in the direction of tensile loading straighten orthogonal yarns undergo additional crimping. This phenomenon is often referred as crimp interchange. A strain rate dependent stiffness, strength and failure strain is exhibited by Twaron and Kevlar fabrics [57, 58]. While the stiffness and strength increased with strain rate, failure strain decreased, with brittle failure at high strain rates and a combination of brittle failure and plastic deformation at low strain rates. The energy absorption at high strain rates is significantly lower than at low strain rates. This is attributed to the intermolecular slippage and plastic flow at low strain rates resulting in more energy absorption.

Fibers directly underneath the projectile and at yarn cross over points are expected to have substantial transverse stresses [59]. The transverse stresses may be amplified depending on specific boundary conditions, for example multi-layer impact scenarios with surrogate backing which constrain the yarn out-of-plane displacements [60]. However there is limited investigation of transverse properties of ballistic fabrics in the literature. A nonlinear force displacement response with increasing stiffness is observed for QS transverse compression tests on 28 plies of Kevlar KM2 fabric [60]. A bilinear load displacement response is observed during a static transverse indentation of Kevlar fabrics with an initially compliant response due to the decrimping of yarns and a stiffer response due to the stretching of yarns [56, 61]. In-plane fabric shear necessary for homogenized membrane fabric model is typically determined through a picture frame test [62-64].

The fabric length scale impact experiments reviewed in this section indicate complicated failure modes and mechanisms observed including transverse shear and compression of the initial layers, pyramidal wave propagation, yarn pull out, inter-yarn friction, progressive fiber failure, slipping through of the sharp nosed projectiles, and fibrillation. Other fabric length scale mechanical characterization experiments discussed above also reveal complicated mechanisms occurring at lower length scales such as crimp interchange, strain rate dependent properties and failure. Lower length scale modeling and experiments are needed to better understand these mechanisms. For instance to study the effect of different fabric architecture and inter-yarn friction, yarn length scale modeling resolution is required. This, in turn, necessitates yarn length scale experiments to characterize the yarn behavior needed as input to the numerical models.

Yarn length scale experiments

A yarn consists of a bundle of minimally twisted fibers with fiber counts in the range of 100-10,000. The yarns differ in denier, number of filaments and tenacity. Denier is yarn weight in grams per 9000 m [11] and tenacity is force in grams required to break a yarn [19]. For example, a Kevlar KM2 600 denier yarn consists of 400 individual fibers. The transverse impact experiments reported in the literature are at the yarn length scale [26] and fabric length scale [40] as it is extremely challenging to capture real time information at the fiber (micron) length scale. The dominant role and contribution of principal yarns (yarns directly in contact with projectile) to energy absorption and projectile deceleration is reported by several researchers [17, 65]. Fibers belonging to the principal yarns directly underneath the impact and at yarn cross overs are subjected to significant transverse compressive stresses.

The current state-of-the-art experimental capabilities in yarn transverse impact testing does not have the spatial resolution to track individual single fiber (KM2 fiber is 12.0 μm in diameter) deformations in real time. The high speed camera imaging allows measuring transverse wave speed and the failure mode. The transverse wave propagation speed is measured assuming the yarn to be homogeneous (that is individual fiber-fiber interactions are not considered).The transverse wave velocity from Smith theory (Equation 2) is shown to match approximately with the experimentally measured velocity for different yarns including KM2, Dyneema HB80 and PBO [28]. The experimentally measured Euler transverse wave speeds and transverse wave angles increase nonlinearly with impact velocity as shown in Figure 5(a) using a wave speed of 7639 m/s for Kevlar KM2 yarns [26]. The influence of the presence of 20% matrix in a UHMWPE Dyneema HB80 strip is argued to slow down the wave speed $c = \sqrt{\frac{1}{M}\frac{dT}{d\varepsilon}}$ by a factor of 0.91, where M is the mass per unit length, T is the tensile force and ε is the strain [39]. This wave propagation information can be used to validate the properties of a yarn length scale model. Most recently Song and Lu [66] noted that fibers are impacted progressively along the thickness direction (see Figure 5(b)) based on their KM2 yarn transverse impact experiments. They further noted that "yarn behaves simply as a group of individual fibers instead of a solid component bundling all fibers". While the transverse wave in aramid yarns appear to make a sharp transition at the

horizontal direction for a sharp edge impact (fragment simulating projectile (FSP)), curvature and bending of the fibers are observed for a blunt nosed projectile impact as shown in Figure 5(c) and (d).

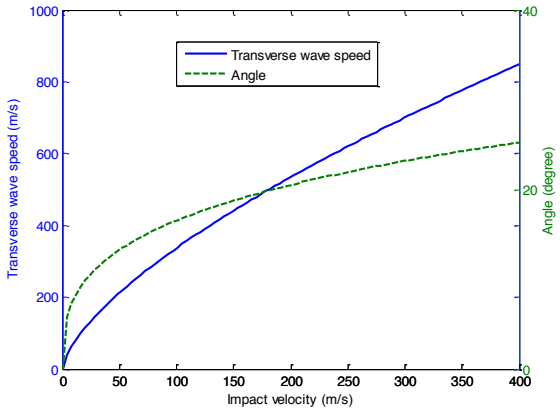

(a)

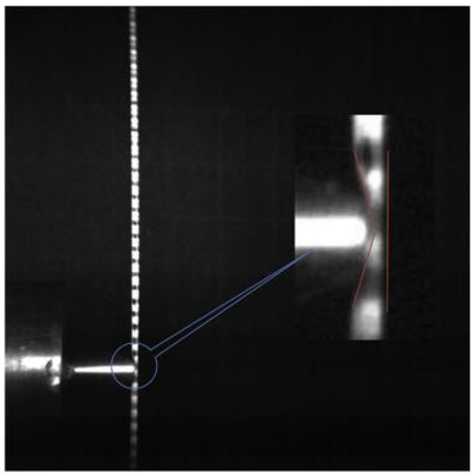

(b)

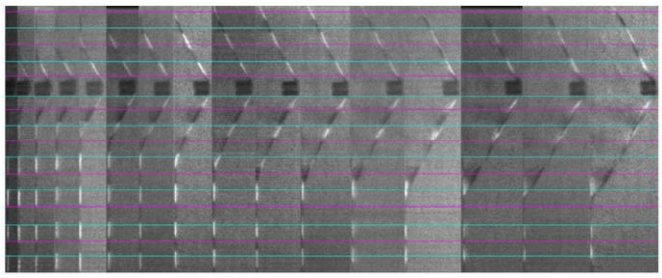

(c)

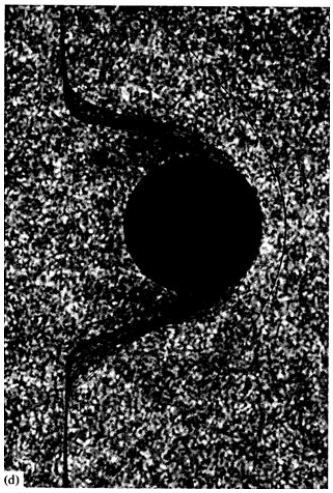

(d)

Figure 5. (a) Transverse wave speed (Equation 3) and wave angle (Equation 4) for KM2 (b) KM2 yarn transverse impact (figure courtesy Song and Lu [66]) (c) FSP impact (figure courtesy Chocron et al. [28]) (d) Blunt nose impact (figure courtesy Bazhenov et al. [67])

The yarns failed in a transmitted stress wave mode (after the development of transverse V wave) for low impact energies or a shear "plug" mode for high impact energies [68]. It is also found that aramid fibers failed in fibrillation and UHMWPE fibers failed in shear with shear bands and melt damage. Aramid yarns showed increased specific energy absorption at low impact energies than at high impact energies due to increased fibrillation at low impact energies. However UHMWPE yarns showed an opposite trend with higher energy absorption at higher impact energy. In general, experimentally observed breaking velocity of yarns is much smaller than the theoretical breaking velocity [27]. This is attributed to the projectile-fiber interactions, multi-axial loading, progressive and statistical nature of fiber failure which is not accounted in the analytical solution as discussed earlier. Other transverse impact experiments on yarns include the work by Field and Sun [69], Heru Utomo and Broos [70] and Bazhenov et al. [67].

The QS yarn behavior and strength has been investigated by several researchers [48, 71-74] that can feed into homogenized yarn resolution models discussed later. In general, a linear behavior is

displayed by the yarns and a lower strength is observed at higher gage lengths. The yarns also exhibit a statistical distribution in strength due to inherent strength distribution and misalignment of the fibers leading to progressive filament failure at different locations of the gage length [72]. Dynamic yarn tensile tests are often conducted using a split Hopkinson tension bar. Dynamic tensile testing of yarns indicated weak dependence of strength on strain rate (800 s^{-1}) for Kevlar and a strong dependence for Twaron and Zylon fibers [75]. In another study, an increase in modulus, strength and failure strain is observed at a strain rate of 480 s^{-1} compared to QS for Twaron yarns [73]. Additionally, for Twaron yarns, longer fibrils are observed at low strain rates and shorter fibrils at high strain rates which are explained due to inter-chain slippage secondary bond failure and primary bond failure respectively [73]. Similar increase in the tensile properties is observed for Kevlar 49 yarns for strain rate in the range of 20 s^{-1} to 100 s^{-1} [74]. The strength, strain energy and failure mechanism of poly para-phenylene terephthalamide (PPTA) and UHMWPE fiber bundles are strongly dependent on the fiber microstructure and morphology than the strain rate [76]. Fibrillation is the failure mechanism for PPTA fibers at both low and high strain rates whereas crazing is the dominant mechanism for UHMWPE fibers at high strain rates. Some yarns show strong rate dependent tensile properties while others show weak dependence. These results clearly show the properties strongly depend on the microstructure and morphology of the fibers that requires further investigation.
QS [5, 77-82] and dynamic yarn pull out [83, 84], influence of twist [85] and inter yarn friction [86] studies are other experiments conducted at the yarn length scale to understand the energy absorption during impact. Most of the yarn transverse impact experiments reported in the literature are focused on determining the transverse wave velocity and the 'V' angle from the images obtained. Both the transverse impact and mechanical yarn characterization experiments treated yarn as a homogeneous material. However the experiments indicate the failure modes and mechanisms are governed by fiber-fiber interactions, fiber properties and microstructure. To better understand the fundamental mechanisms during impact, research in the direction of understanding fiber-fiber interactions, failure initiation and propagation, and post-failure investigation is needed.

Fiber length scale experiments

High performance polymer fibers lend themselves to ballistic applications due to their superior specific strength, specific modulus and energy absorbing properties. The properties of an aramid (Kevlar KM2) and a polyethylene (Spectra 900) single fiber are listed in Table 2. These fibers, in general, exhibit transverse isotropy with linear elastic behavior in longitudinal tension and nonlinear inelastic behavior in transverse (diametral) compression [87, 88].

Table 2. Properties of Kevlar KM2 [88], [89] and Spectra 900 single fiber [90]

Property	**Aramid (Kevlar KM2)**	**Polyethylene (Spectra 900)**
Density (g/cm3)	1.45	0.97
Diameter (μm)	12.0	38.0
Axial tensile modulus E_3 (GPa)	84.62	117.21
Transverse modulus E_1 (GPa)	1.34	-
Longitudinal shear modulus G_{13} (GPa)	24.40	-
Poisson's ratio ν_{31}	0.60	-
Poisson's ratio ν_{12}	0.24	-

Axial tensile strength	3.88	2.60
Elongation (%)	4.50	3.60
Axial compressive strength	0.68	-
Longitudinal wave speed (m/s) $c = \sqrt{\frac{E_3}{\rho}}$	7639	10992

There is an increasing interest to understand the strain rate dependent tensile response of ballistic fibers as they are subjected to high strain rates during impact. QS and dynamic single fiber tensile tests [88, 91-94] are often used to characterize the fibers in axial tension. Most of the recent researches on dynamic fiber tensile testing are conducted using a miniaturized Kolksy bar [88]. The PPTA fibers, in general, show a strain rate dependent strength behavior. Additionally, the fibers exhibit gage length dependent strength, statistical distribution of strengths and diameter dependent strength at high strain rates [95, 96]. Kim et al. [95] measured an increase of 14% average tensile strength at HSR loading (103 s^{-1}) than QS loading for Kevlar 29 fibers. However Cheng et al. [88] showed the longitudinal tensile properties of Kevlar KM2 fibers are insensitive to strain rates. Fibrillation is observed as the main failure mode for both QS and HSR loading. Figure 1(h) shows the image of a fibrillated Kevlar KM2 fiber subjected to QS tension. UHMWPE fibers also display a strain rate dependent strength behavior [97]. For instance, Dyneema SK76 fibers exhibited an overall increase in tensile strength with strain rates (1 s^{-1} to103 s^{-1}). A transition from viscoelastic to elastic behavior is exhibited by the fibers from low to high strain rates with fibrillation at high strain rates. Even with these experiments failure initiation and propagation leading to final failure of a single fiber is not well understood. Similar to yarn axial tensile results, these single fiber results also show that the properties strongly depend on the microstructure and morphology of the fibers that require further investigation.

Researchers recognized the importance of understanding deformation modes (see Figure 6) other than axial tension that are occurring during an impact. Several researchers have investigated the single fiber transverse compression response of Kevlar fibers including Kawabata [98], Singletary et al. [99, 100] and Cheng et al. [87] and limited investigations on UHMWPE fibers [101]. The experimental results reported by these researchers indicate fibers exhibit nonlinear and inelastic response under large compressive strains. While Cheng et al. [87] compared this nonlinear behavior to the Mullin's effect in rubber materials, Singletary et al. [100] attributed the observed force deflection pattern for staple fibers as cracking of the fiber, followed by closing of the cracks under compression that leads to the overall inelastic response. They also hypothesized transverse yielding followed by fibrillation for the force deflection pattern observed for 1.5 denier Kevlar 29 fibers. These fibers exhibit nonlinear inelastic behavior in transverse compression with a small transverse elastic limit [102, 103]. Wollbrett-Blitz et al. [103] determined the transverse compression elastic limit for Kevlar 29 fibers as 0.25 N/mm below which no permanent deformation was observed. However, most of the finite element (FE) modeling reported in the literature at different length scales (fiber, yarn and fabric) assumes a transversely isotropic linear elastic behavior for the material. The role of inelastic transverse compression fiber behavior during impact is not well understood.

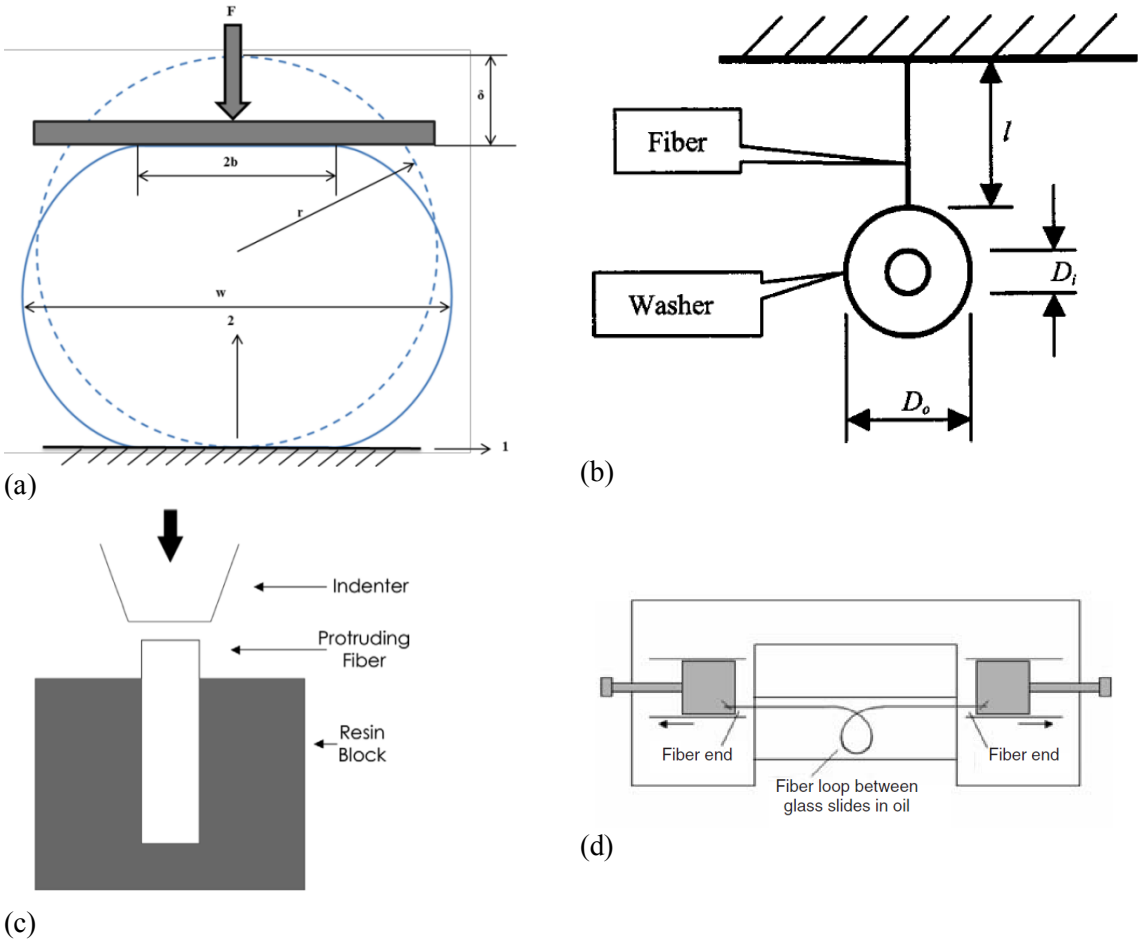

Figure. 6. Schematic of (a) single fiber transverse compression (b) torsional pendulum longitudinal shear [88] (c) micro-compression [104] (d) elastica loop test [89]

The general approach adopted to estimate the transverse modulus is to use the load-displacement measurements in conjunction with the elastic small strain analytical solution based on the Hertzian contact models between parallel plates [105, 106]. An elastic modulus of 1.34 $\pm$ 0.35 GPa and 2.45 $\pm$ 0.40 GPa is estimated for KM2 [87] and Kevlar 29 [99] fibers respectively. Both geometric and material nonlinearities are embedded in the material response requiring the measurement of contact width to determine the accurate material behavior. However the difficulty associated with the measurement of contact width for smaller fiber diameters is noted in [87, 107]. For larger fiber diameters Pinnock et al. [108] estimated the transverse elastic moduli and Poisson's ratio using the analytical solution for diametral compression [109] and contact width [106]. The observed force displacement behavior and large residual strains in transverse compression can be a significant energy absorption mechanism in ballistic impact applications. Although there is some understanding of the QS transverse compression response of fibers, the HSR response and the role of transverse properties during impact is not well understood.

The analytical treatment of classical theory, discussed earlier, assumes axial tension is the only force in the fiber. However, experimentally observed curvature in the transverse deflection of a fabric and weaving process may induce axial compression and shear. Single fiber axial compressive moduli and strength for different high performance fibers including Kevlar KM2 (0.68 GPa) is reported in Leal et al. [89] (see Figure 6(c)). Fibers are found to have different modulus in compression than in tension (Ec/Et = 0.61 for KM2). Kevlar KM2 fibers in elastic

loop experiments (see Figure 6(d)) loaded in flexure are damaged in compression through the formation of kink-bands that causes fibrillation of the fiber microstructure. Micro cracking and fibrillation due to kink bands in Kevlar KM2 fibers are also observed resulting in a 10% loss in tenacity [110]. The aramid Kevlar fibers also have finite longitudinal shear moduli, 29 GPa for Kevlar 29 [111] and 24.4 GPa for Kevlar KM2 [88] based on torsional pendulum experiment [112] (see Figure 6(b)). While most of the literature on the impact of flexible textile composites focuses on tension (axial loading), the consideration of bending and its effects is limited.

Multi-axial stress state of the fiber is expected under ballistic conditions. However there is a limited study on the multi-axial loading response of fibers in the literature. Cheng et al. [87] investigated the response of Kevlar KM2 fibers for bi-axial loading conditions by conducting both longitudinal tensile tests after transverse compression and transverse compression tests after longitudinal tension. They reported insignificant degradation of tensile strength after transversely compressing the fibers to a nominal strain of 0.48 thus allowing the fibers to resist impact loading. Their results on the latter tests indicated longitudinal pre-tension increases the transverse stiffness for nominal strains greater than 0.1. In a later study Lim et al. [96] reported a reduction of about 10% tensile strength (tested at a strain rate of 1500 s^{-1}) for Kevlar and Kevlar 129 fibers after transversely compressed to about 80% of the fiber diameter. They also reported a significant 50% reduction in tensile strength for imperfectly compressed fibers due to misaligned grips. The effect of fibrillation caused by transverse and axial compression on longitudinal shear is not well understood. A finite longitudinal shear stiffness results in a flexural wave during impact and is discussed later.

The effect of twisting of fibers caused by weaving on their strength is recently studied by longitudinal testing after pre-twisting [113]. The study indicates at low and intermediate rates, the Kevlar KM2 fibers retained 95% of its tensile strength for a preloaded shear strain of 0.15. However for shear strains greater than 0.15 a drastic reduction in the tensile strength of the fibers (30% retention in strength at a shear strain of 0.45) is observed due to the surface flaws. A 20% decrease in strength for warp fibers at all high strain rates compared to unwoven (virgin) fibers and a 35% decrease in strength at QS strain rate [114] is observed. Hudspeth et al. [115] also observed similar reduction in tensile strength of Dyneema SK76 fibers subjected to torsional strains and developed a biaxial torsion-tension failure surface. The tensile strength of pre-torsioned fibers is found to be slightly higher at high strain rates than QS loading. These initial experimental studies clearly show the significant effects of multi-axial loading on failure and may serve as input to fiber-level resolution models to accurately predict failure.

Hudspeth et al. [116] examined the failure surfaces of KM2 and Dyneema® SK76 single fibers subjected to different indenters and failure angles (range of 0-50 deg) including razor blade, 0.30 caliber FSP and a round indenter. They observed a shear failure with minimal axial splitting of the fiber for a razor blade indenter and a fibrillation dominated failure for a round indenter for all tested angles. The FSP indenter showed a transition in the fracture surface from fibrillation failure at low angles to shear failure at high angles. Their study also showed approximately constant failure strain for razor blade and round indenters whereas a decreasing failure strains for the FSP indenter with increasing angles. Hudspeth et al. [117] showed a reduction in the KM2 fiber failure strain due to multi-axial stress state and local stress concentration induced by the fiber angle around the FSP indenter.

Although traditionally fiber failure during impact is thought to be tensile dominated, recent research as reviewed in this section looked at other deformation modes including transverse compression, longitudinal shear and multi-axial loading. Characterization of fibers at different loading conditions and strain rates are essential to understand and accurately predict fiber failure during impact. However there is limited research on the strain rate dependent multi-axial loading response of ballistic fibers. One of the reasons is the fiber length scale experiments are challenging due to the associated micron length scale and short time scales. Numerical modeling can help not only to understand the complicated experimental results but also guide the specimen

design for the development of new experimental methods. Fibrillation is a predominant failure mode observed not only in single fiber testing but also in dynamic yarn tensile testing and fabrics subjected to impact. The fiber microstructure needs to be studied to better understand this failure mode.

Ballistic fibrils

The fibrillar core-shell structure of Kevlar aramid fibers based on PPTA has been studied by various researchers [118, 119]. An atomic force microscopy (AFM) phase image of a Kevlar KM2 fiber obtained by McAllister et al. [120] is reproduced in Figure 2. The fibril diameters are in the range of 100-200 nm for Kevlar 49 [121] fibers and 10-50 nm for Kevlar KM2 fibers [120]. Nanoindentation techniques are used to characterize the 3D properties of Kevlar KM2 [119, 122] considering the influence of fibril level heterogeneity on properties. The local compressive elastic moduli are dependent on the number of fibrils loaded by the nano-indentor. Using this technique, an indenter size-independent value of 6.2 ± 1.0 GPa is measured for the local transverse modulus. The measured local transverse modulus is about four times higher than the transverse modulus (1.34 GPa) measured at the fiber length scale (see Table 2). This is because the local modulus is measured using the unloading slope of a number of fibrils that were permanently deformed. It should also be noted, in transverse compression at the fiber length scale, the fiber displays negligible strain recovery upon unloading. Using similar nano-indentation techniques Cole and Strawhecker [123] reported local mechanical properties for four fibers including KM2Plus, Twaron, AuTx, and Dyneema.
The nanoindentation and nanoscratch [124, 125] studies are also important to understand the energy absorbing mechanisms in particle impregnated fabrics using shear thickening fluid [126], silica nanoparticles [56, 127] and carbon nanotubes (CNTs) [128] among others to improve the impact performance. These studies use probes that effectively mimic the contact in particle-fiber and reveal the effects of fundamental particle-fiber interactions on the energy dissipative mechanisms such as friction and particle gouging. For instance, a number of fibrillar deformation mechanisms in KM2 were identified to optimize the specific energy of indentation and scratching such as transverse compression of fibrils, axial fibril tension and inter-fibril shear and friction [124]. The apparent friction (defined as the ratio of lateral scratch force to normal indentation force) is reported [120] to increase up to ~300% higher than the Kevlar yarn-yarn friction of 0.2-0.3. Through these studies, apparent fiber-fiber and yarn-yarn friction were identified as the key energy dissipative mechanisms due to increased apparent friction associated with particle gouging.
UHMWPE is made up of extremely long chains of polyethylene (monomer unit > 250,000 per molecule) with a hierarchy of sizes. Macro-fibrils [129] consist of bundles of micro-fibrils which in turn are composed of bundles of nano-fibrils. Nano-fibrils consist of stacks of crystallites separated by thin non-crystalline plates, portions of which are spanned by inter-crystalline bridges giving a shish-kebab structure [130]. Polyethylene ballistic fibers exhibit a shish-kebab crystalline structure reported through AFM characterization by Strawhecker and Cole [131].

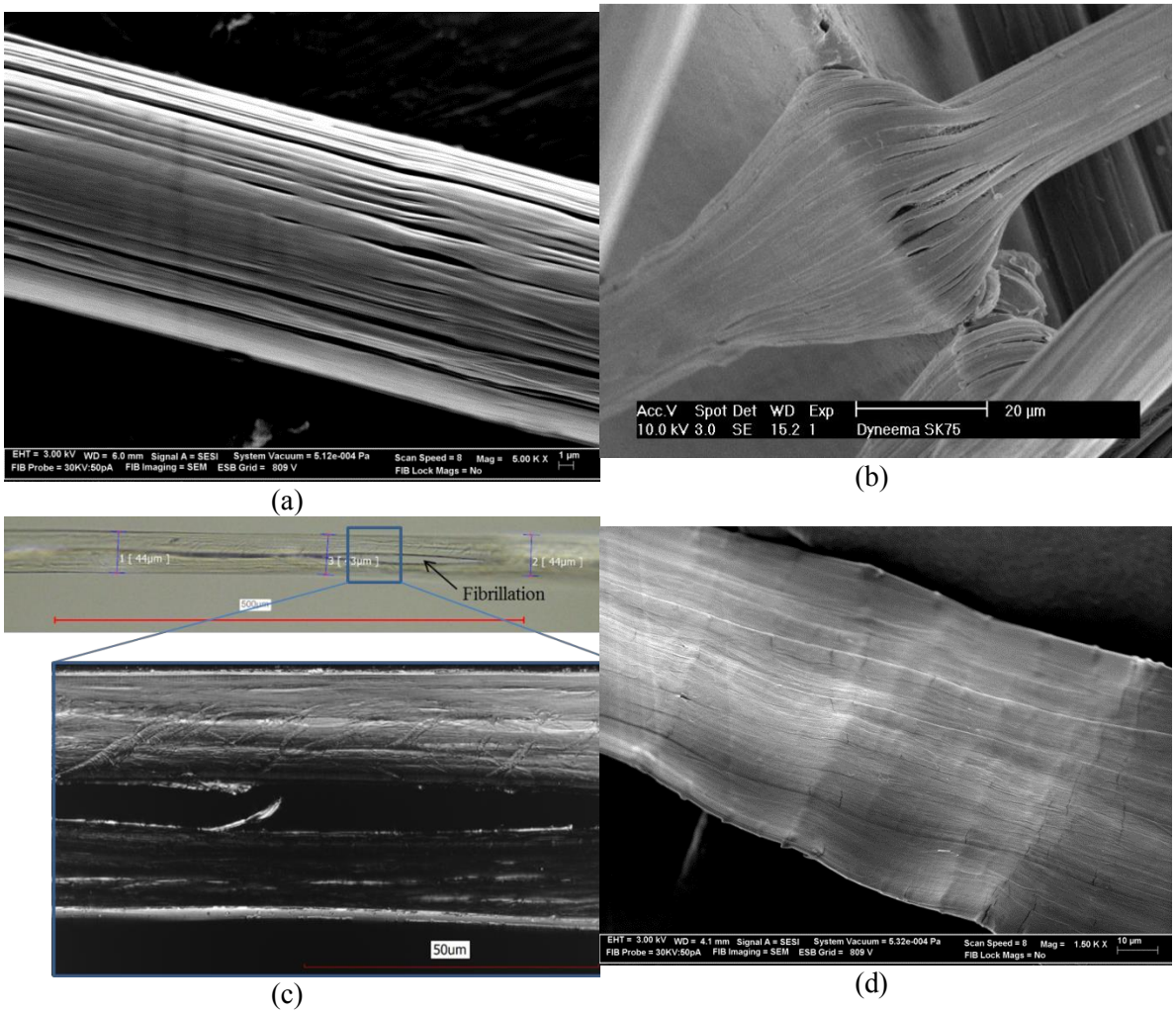

(a) (b) (c) (d)

Figure 7. SEM picture (a) Dyneema® SK76 single fiber (b) Dyneema® fiber deformed by a razor blade (figure courtesy Marissen [132]) (c) KM2 fiber compressed at 77% nominal strain (d) Dyneema® SK76 fiber compressed at 71% nominal strain

It was mentioned earlier that post failure investigation of impacted fabrics showed deformation and failure modes including permanent transverse compressive deformation, fibrillation and transverse shear (cutting) failure. Aramid and UHMWPE fibers can sustain a large amount of transverse compressive strain likely due to their fibrillar network. Figures 7(a) and (b) show scanning electron microscopy (SEM) picture of a Dyneema® SK76 single fiber and a Dyneema® fiber deformed by a razor blade respectively. Fiber is seen to spread along the length of the blade. When subjected to transverse compression, KM2 and Dyneema® SK76 fibers spread to a great extent, compressed width to diameter ratio attaining 3.5 and 4.5 respectively at ~70% nominal strains as shown in Figures 7(c) and (d). These lower length scale experiments at the fiber and fibril level provide insights into the deformation and failure modes that occur during impact and allow for the design of new materials with improved properties. For example, nanoindentation studies[124] indicated highest levels of fiber-fiber friction is achieved with a minimum particle size which then becomes a material design parameter. These experiments also clearly indicate the presence of multi-axial loading and the importance of accounting them in the modeling failure criterion to accurately predict failure.

Modeling of Fibrils, Fibers, Yarns, Single Layer and Multi-Layer Fabrics

Validated numerical models with predictive capability are valuable engineering tools for the design and development of protective systems and to gain insights into the mechanisms governing the impact response. Mechanical characterization experiments at different length scales and strain rates are imperative in the development of high fidelity numerical models. Finite element (FE) modeling using commercially available explicit FE codes is the most common numerical modeling technique to predict the impact response.

Fabric length scale FE modeling of ballistic fabrics

Most of the fabric length scale modeling in the literature looked at comparing the model predictions of projectile residual velocity to the experimental data. Unit cell representative volume element (RVE) techniques based on shell element modeling of fabrics have been adopted by various researchers [133-136] (see Figures 8(a) and (b)). The approach here is to model fabric at the continuum scale accounting for the yarn interactions through contact forces computed from equilibrium at the cross overs with zero through thickness stress and strain. One of the challenges for membrane modeling approaches is to develop constitutive models that accurately describe the lower length scale deformation mechanisms. A membrane element model [137] with viscoelastic and strain rate dependent behavior of the Twaron fabric showed good agreement between the numerical and experimental residual velocity. However, the limitations of this approach, as also recognized in [137], include inability to capture mechanisms such as yarn-yarn friction, unraveling of yarns, slipping through of the projectile and woven architecture as shown in Figure 1(b), (c) and (d).
Another approach is to use an empirically based constitutive model (based on fabric level experiments) and model the fabric as an equivalent continuum using shell elements as shown in Figure 8(a) [138, 139]. Yet another approach [61] adopted a classical laminated plate theory to develop a homogenized continuum constitutive model for Kevlar fabrics using 2D plane stress elements in ABAQUS. Other homogenized modeling approaches include the works by Nadler et al. [140], Boljen and Hermaier [141], Grujicic et al. [142] and Erol et al. [143]. Here the fabric in-plane behavior is decoupled from the thickness direction assuming zero out of plane normal stress. Given the significant transverse compressive deformation observed in fibers and also predicted by fiber level models (discussed later), it is imperative for the homogenized models to carry over that information at higher length scales to accurately capture all the sources of energy absorption.

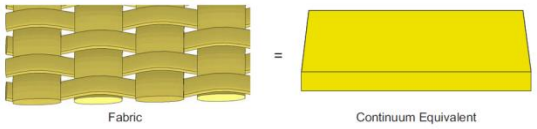

(a)

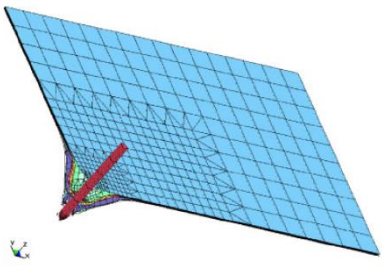

(b)

(c)

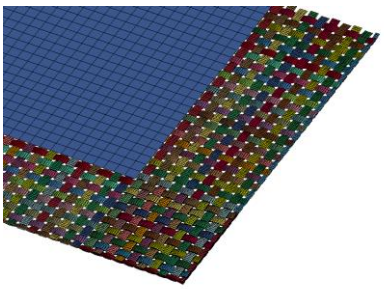

(d)

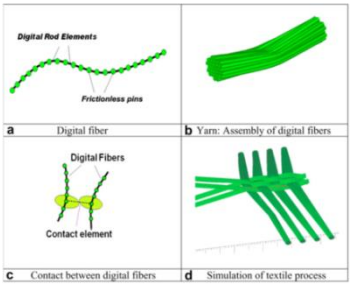

(e)

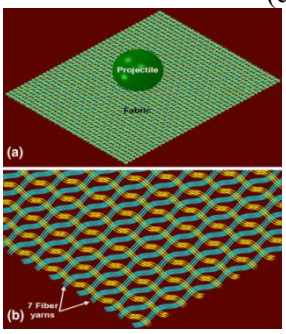

(f)

(g)

(h)

Figure. 8. Modeling at different length scales (a) homogenized fabric model [139] (b) multi-layer fabric impact [133] (c) homogenized yarn length scale [144] (d) combined global/local model [145] (e) digital element method (DEM) [146] (f) fiber-level beam element fabric model [147] (g) fiber-level 3D yarn model [7] (h) comparison of homogenized yarn and fiber-level 3D models [7]

Most of the fabric level modeling does not incorporate the statistical nature of failure. Nonetheless researchers, in general, showed good correlations of model predictions to experiments (for example residual velocity) by introducing calibration parameters such as element removal criterion (erosion strain). Major disadvantage of these modeling approaches is the introduction of parameters that must be fit to impact experiments on each fabric type of interest. A key assumption in homogenized modeling is the problem of interest must have length scales greater than the characteristic yarn spacing (for example, in a plain weave Kevlar K706 fabric, the yarn spacing is 0.75 mm). However impact event is more 'local' and the relation to the characteristic projectile geometry should be taken into account. For instance, a sharp nosed projectile can push through the fibers within a yarn [40] and also a projectile may 'window' through the fabric with no yarn failure [148]. The 'local' nature of impact event is indicated by a small degradation of the tensile properties of yarns that are extracted from a shoot pack away from the impact location [149]. Strain wave reflection, noted by Freeston and Claus [150], at the yarn cross overs can increase the strain level depending on the reflection coefficient. Although length and width of

the fabric is larger than the thickness, impact is a 'local' event causing significant transverse deformation initially which is largely neglected by the continuum scale homogenized approaches. In general, information related to lower length scale mechanisms shown in Figure 1 is lost in homogenization. A holistic multi-scale modeling methodology based on fundamental fiber properties taking into account all the important energy absorbing mechanisms is needed for a truly predictive model. A yarn length scale modeling resolution is needed to accurately predict the yarn pull out and inter-yarn friction mechanisms.

Yarn length scale FE modeling of ballistic fabrics

The early yarn length scale model developed by Roylance [151] and Cunniff et al. [152] modeled the warp and fill yarns with a pair of nodes connected by massless elements with the nodes being coupled through a spring. The transverse compression of the yarn is accounted with a nonlinear spring and bending stiffness with a torsional spring. The yarn crimping significantly slows down the transverse wave speeds and yarn-yarn interaction via coupling springs has a major effect on the ballistic response [152]. Pin-jointed viscoelastic bar elements [153, 154] are used to model the woven aramid fabric and are reported to be able to capture the sliding of yarns and hence wedging of the projectile through the fabric. Pin-jointed approach indicates ballistic response is affected by the coefficient of friction between the yarns [155]. Novotny et al. [156], using a similar approach, concluded the smallest inter-layer gap results in the highest rate of initial specific energy absorption. The pin-jointed approach does not necessarily account for the friction at the yarn cross overs, accurate transverse compression and fiber-fiber interactions.
Meso-scale yarn -evel 3D orthotropic continuum model is developed by explicitly modeling all the yarns in a fabric using solid FE elements as shown Figure 8(c) [48, 144, 157, 158]. Modeling at the yarn length scale using solid elements allows capturing the yarn undulations and inter-yarn friction directly unlike the pin-jointed bar element models. Yarn-level FE models also allow understanding the effect of projectile shape and friction between the yarns during impact [159, 160]. The yarn-yarn friction is reported [144, 161, 162] to play a major role in the energy absorption during impact by increasing the impact load. However it is reported by many researchers that this level of detailed modeling is computationally very expensive.
Researchers also employed multi-scale global/local approaches combining yarn and fabric length scales shown in Figure 8(d) leading to computationally efficient models. Here the woven architecture is modeled around the impact site and fabric length scale (membrane shell elements) away from the impact location [163]. The two length scales are connected by tied interfaces. Rao et al. [164] used 3D solid elements with yarn length scale around the impact site (local) and homogenized solid elements at the far field (global) region. This approach maintained same areal density for both local and global regions and matched impedances across the interfaces to avoid spurious wave reflections. Nilakantan et al. [145] developed hybrid element analysis (HEA) which used solid elements for the yarn length scale around the impact site (local) transitioning into woven shell elements and finally homogenized membrane shell elements for the far field (global) region. This approach leads to a significantly reduced computational expense compared to a full 3D yarn length scale model. Similar yarn length scale and multi-scale modeling approaches include the works by Gogineni et al. [165], Gu [166], Sun et al. [167], Grujicic et al. [142], Jia et al. [168], Yen et al. [169] and Jiang et al. [170]. There is limited yarn level multi-scale modeling that takes into account the fiber-fiber interactions and fiber properties other than axial tension. Zohdi [171, 172] developed a multi-scale model where yarns are modeled as a 2D network. The behavior of the yarn is based on a single fiber behavior taking into account the misalignment of fibers. The random misalignment of fibers results in progressive failure of fibers and also causes difference in the response from yarn to yarn. A similar multi-scale approach adopts a handshaking process between the fabric, yarn and fiber length scales [173, 174].

Though limited, there is some work on probabilistic modeling approach by mapping the statistical strength distribution of yarns onto the yarn length scale FE model to capture the probability of fabric penetration as a function of the projectile impact velocity [175, 176]. For the yarn-level orthotropic continuum FE models all the Poisson's ratios are assumed to be zero and the transverse and shear modulus are assumed to be three orders of magnitude smaller than the longitudinal modulus (and are also an order of magnitude lower than the transverse modulus of an individual fiber) to represent the thread like yarn behavior [177]. An actual 600 denier Kevlar KM2 yarn consists of 400 individual 12 μm diameter fibers. These continuum approaches do not accurately account for transverse compression response of yarns where fiber compression, progressive fiber failure, fiber-fiber contact and friction and fiber spreading within a yarn are important physically observed deformation mechanisms. Again a multi-scale modeling methodology taking into account all the important energy absorbing mechanisms is necessary for a truly predictive model.

Fiber length scale FE modeling of ballistic fabrics

At the fiber length scale Durville [178] developed an enriched kinematical 3D beam model to represent deformation of the fiber cross section considering contact and friction between the fibers. Wang et al. [146] developed digital element method (DEM) to simulate the ballistic impact of textile fabrics wherein the hundreds of fibers in a yarn is represented as an assembly of digital fibers using a few rod elements connected by frictionless pins as shown in Figure 8(e). DEM uses contact elements to model contact between the fibers, the contact stiffness for fiber-fiber compression being calculated using the fiber transverse modulus. A later study implemented nonlinear elastic-plastic model for the contact forces between the digital elements and concluded that energy loss due to fiber transverse plastic deformation significantly affect the ballistic resistance of a fabric [179]. While this approach may be effective in eliminating interpenetrations it does not account for the Poisson's ratio effect in the plane of the isotropy and evolution of a large contact width observed experimentally [96] and contact forces between fibers.
In an approach similar to DEM, 3D beam elements shown in Figure 8(f) are employed to model Kevlar KM2 fibers with a user defined contact algorithm to specify the transverse properties [147]. This approach indicated fiber transverse properties, fiber-fiber and fiber-projectile friction plays a major role in the penetration resistance and hence ballistic performance of the fabric. The most recent studies use independently measured fiber properties to study these interactions. Nilakantan [148] used solid elements to model all the 400 KM2 fibers within a yarn subjected to impact by a hemi-cylindrical projectile and observed flattening and spreading of fibers. At the impact velocities considered (100-120 m/s) the models predicted a spreading wave that propagated along the length of the yarn resulting in progressive spreading of the fibers. The models also predicted the projectile residual velocity being sensitive to the transverse and shear properties. However the finite element discretization used for fibers in [148] is not adequate to capture significant deformations in transverse compression at experimental yarn breaking speeds. None of these numerical approaches have been experimentally validated through direct correlation with transverse compressive loading of a single fiber.
Sockalingam et al. [180, 181] developed fiber length scale FE models to understand the complicated yarn transverse impact experimental results. To gain insight into the fiber-level mechanisms, they systematically studied the QS and dynamic compressive response of single fiber and yarn by explicitly modeling all 400 fibers (of diameter 12 μm) in a 600 denier KM2 yarn with the mesh discretization determined from the single fiber study. The study revealed a large extent of fiber spreading due to the fiber-fiber contact interactions. The significant role of fiber-fiber contact in spreading, frictional interactions and deformation of individual fibers predicted by the model were consistent with experimental observations. Comparison to a homogenized yarn model

indicated the need for a nonlinear material model to accurately capture the transverse compression response.

A study by Sockalingam et al. [182] on single fiber transverse impact using a 3D FE model predicted a dispersive flexural wave mode due to the finite longitudinal shear modulus of the KM2 fiber. The FE model predictions were consistent with an analytical solution derived based on the theory of flexural waves in thin rods for an infinite Euler-Bernoulli beam subjected to a constant velocity impact at its mid span. They further studied the yarn transverse impact [7] at the fiber length scale by explicitly modeling all the fibers in a yarn using a 3D FE model shown in Figure 8(f) and (g). At the short time scale the fibers undergo significant transverse compressive deformation (~80% true compressive strains at 500 m/s impact) sufficient to induce fibrillation with little spreading resulting in multi-axial stress states as shown in Figure 9. The fiber-level model revealed complicated dynamic fiber kinematics and mechanisms with a dispersive flexural wave and a spreading wave. The flexural wave results in bending of fibers and significantly higher axial stresses under the impact and at the clamped end compared to a homogenized yarn level model. The curvatures due to bending in the fiber are significant enough to cause axial compressive kinking and fibrillation under the impact. The fibers experience multi-axial stress states, non-uniform loading and progressive failure depending on their spatial location. The multi-axial loading, flexural wave induced axial compression, fiber bounce, progressive loading are mechanisms that may explain experimentally observed lower breaking speed for yarns than classic analytic solution. However, the model does not account for the misalignment and statistical failure of fibers.

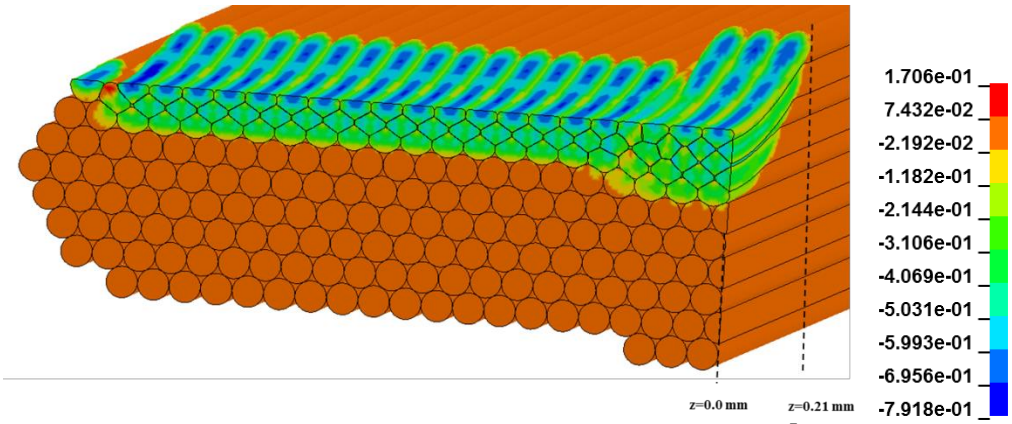

Figure 9. Contours of short time scale compressive strains at 500 m/s impact[7]

There is limited investigation of fiber length scale modeling in the literature due to the computational intensity of the models. However, with advances in the computing power more research is being focused on the lower length scales to understand the fundamental deformation and failure mechanisms. Most recently Recchia et al. [183] developed a filament model of 600 denier KM2 yarn incorporating different levels of twists in the fibers using beam elements. Up to a certain level of twist (3 twists per inch (TPI)) the yarn tensile strength is found to increase due to outer filaments being stressed more than the inner ones whereas a high level of twist (10 TPI) reduces the ultimate tensile strength due to high local stress concentrations. Xia et al. [174] noted that misalignment of fibers affects the stiffness and failure of yarns. Fiber level modeling resolution allows studying the effect of diameter and number of fibers, statistical strength distribution, degree of twist and so on, for different loading scenarios and hence on the impact response.

Fiber level modeling indicates progressive failure of fibers, significant transverse compression and curvature induced compressive kinking leading to fibrillation failure. There is also

experimental evidence on fibrillation of fibers subjected to transverse compression, compressive kinking and axial tension. To better understand fibrillation and fibril failure, a lower length scale modeling approach is necessary.

Inelastic material response

Most of the modeling work discussed in this section so far assumes an elastic behavior for the material at different length scales (fabric, yarn and fiber). However the fiber transverse compression QS experimental results clearly indicate a very small elastic limit (1.25% strain for KM2 fiber) and an inelastic behavior of the material with negligible strain recovery upon unloading [184]. The transverse compressive response of the fibers at high rates of deformation is not well understood. The role of this inelastic transverse compression behavior and the associated energy absorption during impact is also not well understood. The inelastic compressive behavior may result in dissipative effects and may influence the evolution of axial strains in the material and hence its failure. Therefore to accurately predict energy absorption and failure, future work must consider the inelastic material constitutive behavior at high rates of loading.

Fibril length scale molecular dynamics (MD) modeling of ballistic fibrils

Recently there has been an increasing interest to characterize the material properties under dynamic loading using molecular simulations due to the advances in computational power. Simulations with ab-initio principle are more accurate but computationally very expensive even with state-of-art computational capability. Classical MD simulations which solve Newton's equations of motion [185] are less expensive. The empirical force fields used in the classical MD simulations are derived based on experimental and ab-initio calculations. The accuracy of the simulation depends on the choice of force field for atomic interactions in the system. For computational efficiency in both the length- and time-scale, united atom and coarse grain approaches are adopted in the classical molecular simulations [186]. Since experimentation at the fibril length scale is very challenging, molecular simulation is an excellent alternative tool to characterize the materials and get insight into the behavior of the materials under impact conditions.

Molecular simulations on Kevlar reported in the literature mainly studied the elastic and strength properties under tensile and compressive loads rather than dedicatedly focusing on the multi-axial loading and ballistic performance. Recently, Grujicic et al. [187-189] studied the properties of PPTA using classical MD simulations. They used non-reactive force field COMPASS (Condensed-phase Optimized Molecular Potentials for Atomistic Simulation Studies) [190] to represent the atomic interactions. In one study [187], they investigated the effects of microstructural and topological defects such as chain ends, inorganic-solvent impurities, chain misalignments and sheet stacking fault on the strength, ductility and stiffness of PPTA fibril. Presence of these defects decreases the mechanical properties of PPTA fibrils. However, some specific properties are found to be particularly sensitive to the presence of certain defects. For example, longitudinal tensile properties are found to be the most sensitive to the presence of chain ends, in-sheet transverse properties to the presence of chain misalignments, and cross-sheet transverse properties to the presence of sheet stacking faults. From the fibril model properties, they proposed fiber and yarn level material model considering fibril level crystallographic and morphological defects [188].

In another study [189], they investigated the effects of prior-axial compression and torsion on the longitudinal tensile behavior of PPTA fibrils and the role of various micro-structural/topological defects affecting this behavior. In the presence of defects, prior-axial compression and torsion degrades the longitudinal tensile strength. However, prior-axial compression and torsion do not degrade the longitudinal tensile strength of a perfect PPTA fibril since there is no permanent change in the PPTA micro-structure after removal of these pre-loads. Determining strength

properties using the non-reactive force fields is questionable since these force fields do not capture the bond breaking phenomena. Therefore analyzing the structure and mechanical properties of Kevlar with reactive force field is necessary to further our understanding on the deformation and failure mechanisms.

There is some evidence in the literature indicating the presence of compressive kink bands in polymer composites under ballistic impact [191] indicating the multi-axial loading. The curvature predicted by the single fiber transverse impact model [182] is physically induced by wrapping single KM2 fibers around a Boron fiber with a curvature of ~ 18/mm. A characteristic kink band density of 70 per mm and an approximate angle of 60^o are observed. Figure 10(a) shows an SEM picture of the kink bands [192]. MD model of Kevlar subjected to axial compression, as shown in Figure 10(b), indicates that kinking initiates through the lateral deflection of the Kevlar chains in a direction normal to the plane containing the hydrogen bonds. While MD models predict kinking at high rates of loading further experimental studies are needed to understand the kink band formation at high rates. However the ratio of the characteristic distance between the kinks to the model thickness is found to be in good agreement with the experiment.

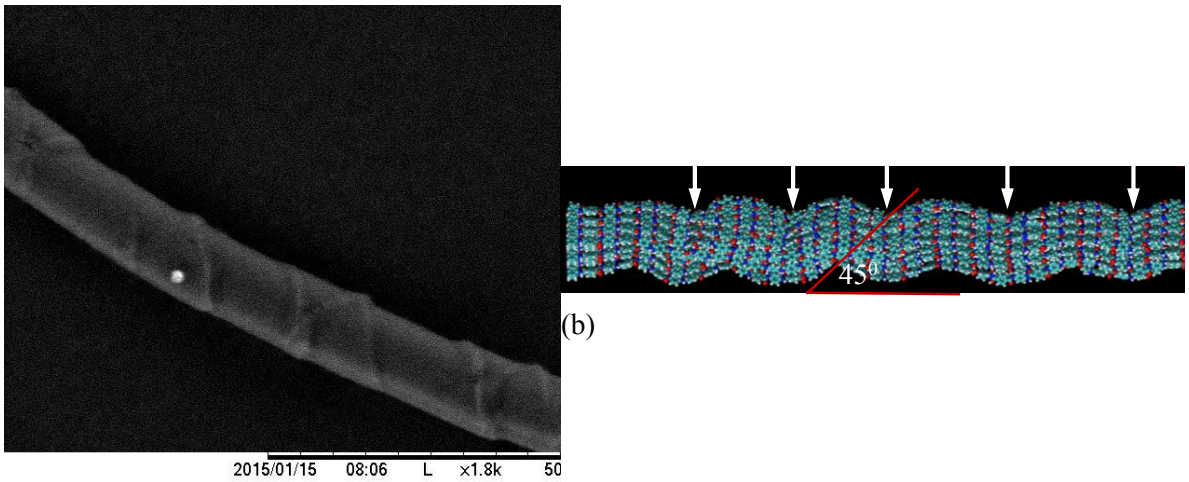

(a) (b)

Figure 10. (a) SEM picture of kink bands on a single KM2 fiber[192] (b) Kinking predicted by MD model[192]

Fibrillation of fibers under impact is a predominant failure mechanism which is not well understood. Recently Mayo and Wetzel [193] studied the cut resistance and failure of single fibers and report significant deformation, delamination and progressive fibril failure of Kevlar fibers depending on the blade angle. Thomas et al. [194] and Lomicka et al. [195] used MD simulations to predict the properties of Kevlar fibrils. The MD models predicted higher elastic modulus in tension than the experimental values which they attributed to the lack of defects in the model. MD models not only provide insight into how molecular and fibril level properties may affect the fiber properties but also assist in designing materials with improved properties. For instance, Thomas et al. [194] used fragments of CNTs along with Kevlar fibrils in their MD simulations and predicted a 10% higher tensile failure stress compared to a Kevlar only system. As discussed earlier inter-fibrillar shear is an important mechanism during nanoindentation and in energy absorption associated with particle-impregnated fabrics. However, modeling efforts to investigate and better understand this mechanism is scant. Recchia et al. [196] developed a nanoscale FE model to account for the fibrillar microstructure of Kevlar fibers to predict the axial tensile response of the fiber. They used a cohesive zone model to mimic the inter-fibrillar interaction forces. Based on a parametric study they showed fibril response is strongly dependent on the cohesive

interactions. Alternatively, MD simulations may be used to rigorously determine the inter-fibrillar response which can then be used in fibril-level FE models [197].
Unlike Kevlar, there are numerous molecular simulation studies on polyethylene (PE) [198-203]. Some of them used united-atom and coarse grain approaches to reduce the computational cost. Most of the simulations focused on the characterization of microstructures, elastic and strength properties, thermal properties, and deformation of the bulk amorphous polymer rather than focusing on structural ballistic PE fibers which have a hierarchical structure consisting of crystalline and amorphous phase. There is limited work on characterizing the behavior of the PE fibers under dynamic impact and the associated deformation and damage mechanisms. Mattsson et al. [204] conducted quantum and classical MD simulations of polyethylene under shock compression to study the accuracy of the different empirical force fields. Recently, Chantawansri et al. [205] also conducted shock Hugoniot calculation of polymer using quantum and MD method. They produced the principle shock Hugoniot curve and compared with the available experimental results.

Conclusions

The deformation and failure mechanisms during the ballistic impact of a flexible woven textile fabric are complicated involving multiple length and time scales affected by anisotropic material behavior, projectile geometry-fabric interactions, impact velocity and boundary conditions. This paper reviewed the recent research in modeling and experiments of important mechanisms and deformation modes of these materials (particularly Kevlar and polyethylene) at different length scales and strain rates. Although fiber specific toughness and longitudinal wave speed are important properties affecting the ballistic performance, this review indicates other properties and mechanisms such as fiber transverse compression, longitudinal shear, multi-axial loading response, flexural wave, different longitudinal tensile and compressive moduli, fibrillation, statistical fiber failure and fiber-fiber interactions play a major role in the energy absorption during impact. Important information governing energy absorption is lost while homogenizing to higher length scales. The transverse impact on fabrics requires a multi-scale modeling approach from fibrils to multi-layers. In general, there is limited research reported in the literature on the experiments and modeling of these materials at lower length scales (fiber-level and lower). Some key takeaways based on the review are:

i) Some of the complex mechanisms observed in a fabric length scale impact experiments are: transverse shear and compression failure of the initial layers, pyramidal wave propagation, yarn pull out, inter-yarn friction, progressive fiber failure, slipping through of the sharp nosed projectiles, spreading and flattening of fibers and fibrillation. Lower length scale experiments are necessary to better understand these mechanisms and the associated energy absorption.

ii) Fiber-fiber interactions and progressive fiber failure during the transverse impact of a yarn are not well understood as most of the impact experiments reported in the literature focused on transverse wave speed and angle.

iii) The load transfer and energy absorption mechanisms at lower length scales are not well understood. This understanding will provide opportunities to design better materials to achieve optimum impact performance. There are opportunities to better understand HSR transverse compression response and the role of transverse properties of the fiber during impact.

iv) Fibrillation is an important failure mode for the high performance Kevlar and polyethylene ballistic fibers which is poorly understood. Molecular simulation of fibrils along with nano-scale experimentation may help to provide insights into the failure process.

v) Characterization of fibers subjected to multi-axial loading at different strain rates can improve the predictive capability of the models. This necessitates experiments with multi-axial loading at different strain rates to accurately predict fiber failure.

vi) Most of the modeling approaches do not consider the experimentally observed inelastic transverse compression behavior of the fiber. Future modeling efforts at different length scales must consider this to accurately predict the energy absorption and failure.

vii) Most of the modeling approaches do not incorporate the statistical nature of failure. To improve the predictive capability of the models it is important to incorporate the statistical nature of material failure.

viii) In general, element removal (erosion strain) is used in ballistic impact FE models to model material failure. Erosion strain is used to remove the heavily distorted elements which would otherwise significantly reduce the computational time step. However erosion strain is known to be mesh dependent and can alter the results. To accurately predict failure, mesh objective/regularization techniques and nonlocal approaches such as Peridynamics [206, 207] may be considered.

ix) Modeling at the lower length scales helps understand the responsible load transfer and energy absorption mechanisms. Opportunities exist to understand the effect of the different fiber longitudinal tensile and compressive moduli, fiber misalignment, twist, undulations, statistical strength distribution, strain rate dependent multi-axial failure, transverse permanent deformation and so on. It is also imperative to account for these mechanisms in order to accurately predict material failure.

x) Morphology dependent properties and failure during impact is observed. To develop new protective materials, it would be useful to conduct MD simulations at high strain rates to understand the morphology change in the fiber microstructure and associated energy absorbing mechanisms.

Acknowledgments

Research was sponsored by the Army Research Laboratory and was accomplished under Cooperative Agreement Number W911NF-12-2-0022. The views and conclusions contained in this document are those of the authors and should not be interpreted as representing the official policies, either expressed or implied, of the Army Research Laboratory or the U.S. Government. The U.S. Government is authorized to reproduce and distribute reprints for Government purposes notwithstanding any copyright notation herein

References

1. Kim J, McDonough WG, Blair W, et al. The modified-single fiber test: A methodology for monitoring ballistic performance. *J Appl Polym Sci* 2008; 108: 876-886.

2. Krishnan K, Sockalingam S, Bansal S, et al. Numerical simulation of ceramic composite armor subjected to ballistic impact. *Composites Part B: Engineering* 2010; 41: 583-593.

3. Sharda J, Deenadayalu C, Mobasher B, et al. Modeling of Multilayer Composite Fabrics for Gas Turbine Engine Containment Systems. *J Aerosp Eng* 2006; 19: 38-45.

4. Chocron S, Figueroa E, King N, et al. Modeling and validation of full fabric targets under ballistic impact. *Composites Sci Technol* 2010; 70: 2012-2022.

5. Nilakantan G, Merrill RL, Keefe M, et al. Experimental investigation of the role of frictional yarn pull-out and windowing on the probabilistic impact response of kevlar fabrics. *Composites Part B: Engineering* 2015; 68: 215-229.

6. Nilakantan G, Keefe M, Gillespie Jr JW, et al. An experimental and numerical study of the impact response (V50) of flexible plain weave fabrics: Accounting for statistical distributions of yarn strength. In: *The 1st Joint American-Canadian International Conference on Composites and the 24th Annual ASC Technical Conference, University of Delaware, Newark, DE 19711, USA*, September, 2009.

7. Sockalingam S, Gillespie Jr. JW and Keefe M. Fiber-level tow modeling of Kevlar KM2 subjected to high velocity impact. In: E. Albers, Robert; Beckwith, Scott W.; Cates (Ed.), *SAMPE*, Seattle, WA, USA, June 2-5, 2014.

8. Northolt M and Van Aartsen J. On the crystal and molecular structure of poly-(p-phenylene terephthalamide). *Journal of Polymer Science: Polymer Letters* Edition 1973; 11: 333-337.

9. Northolt M. X-ray diffraction study of poly (p-phenylene terephthalamide) fibres. *European Polymer Journal* 1974; 10: 799-804.

10. Tashiro K, Kobayashi M and Tadokoro H. Elastic moduli and molecular structures of several crystalline polymers, including aromatic polyamides. *Macromolecules* 1977; 10: 413-420.

11. Yang HH. Kevlar aramid fiber. *Wiley*, 1993.

12. Bunn CW. The crystal structure of long-chain normal paraffin hydrocarbons. The “shape” of the< CH2 group. *Transactions of the Faraday Society* 1939; 35: 482-491.

13. Bank M and Krimm S. Lattice-frequency studies of crystalline and fold structure in polyethylene. *J Appl Phys* 1968; 39: 4951-4958.

14. Seto T, Hara T and Tanaka K. Phase transformation and deformation processes in oriented polyethylene. *Japanese Journal of applied Physics* 1968; 7: 31.

15. Bassett D, Block S and Piermarini G. A high-pressure phase of polyethylene and chain-extended growth. *J Appl Phys* 1974; 45: 4146-4150.

16. Prevorsek DC, Kwon YD, Chin HB. Analysis of the temperature rise in the projectile and extended chain polyethylene fiber composite armor during ballistic impact and penetration. *Polymer Engineering & Science*. 1994 Jan 1;34(2):141-52.

17. Cheeseman BA and Bogetti TA. Ballistic impact into fabric and compliant composite laminates. *Composite Structures* 2003; 61: 161-173.

18. Tabiei A and Nilakantan G. Ballistic impact of dry woven fabric composites: a review. *Appl Mech Rev* 2008; 61: 010801.

19. David N, Gao X and Zheng J. Ballistic resistant body armor: contemporary and prospective materials and related protection mechanisms. *Appl Mech Rev* 2009; 62: 050802.

20. Haque BZG and Gillespie JW. A new penetration equation for ballistic limit analysis. *J Thermoplast Compos Mater* 2013: 0892705713495430.

21. Smith JC, McCrackin FL and Schiefer HF. Stress-Strain Relationships in Yarns Subjected to Rapid Impact Loading: Part V: Wave Propagation in Long Textile Yarns Impacted Transversely. *Textile Research Journal* 1958; 28: 288-302.

22. Smith JC, Blandford JM and Schiefer HF. Stress-Strain Relationships. in Yarns Subjected to Rapid Impact Loading Part VI: Velocities of Strain Waves Resulting from Impact. *Text Res J* 1960; 30: 752-760.

23. Mamivand M and Liaghat GH. A model for ballistic impact on multi-layer fabric targets. *Int J Impact Eng* 2010; 37: 806-812.

24. Cole J, Dougherty C and Huth J. Constant strain waves in strings. *Journal of Applied Mechanics*, 1953; 53-SA-4.

25. Wang L. Foundations of stress waves, *Elsevier*, 2011.

26. Song B, Park H, Lu W-, et al. Transverse impact response of a linear elastic ballistic fiber yarn. *Journal of Applied Mechanics* 2011; 78.

27. Walker JD and Chocron S. Why impacted yarns break at lower speed than classical theory predicts. *Journal of Applied Mechanics* 2011; 78: 051021.

28. Chocron S, Kirchdoerfer T, King N, et al. Modeling of fabric impact with high speed imaging and nickel-chromium wires validation. *Journal of Applied Mechanics* 2011; 78: 051007.

29. Leigh Phoenix S and Porwal PK. A new membrane model for the ballistic impact response and V50 performance of multi-ply fibrous systems. *Int J Solids Structures* 2003; 40: 6723-6765.

30. Porwal PK and Phoenix SL. Modeling system effects in ballistic impact into multi-layered fibrous materials for soft body armor. *Int J Fract* 2005; 135: 217-249.

31. Cunniff PM. Dimensionless parameters for optimization of textile-based body armor systems. In: *Proceedings of the 18th international symposium on ballistics*, pp.1303-1310: San Antonio: Texas.

32. Afshari M, Chen P and Kotek R. Relationship between tensile properties and ballistic performance of poly (ethylene naphthalate) woven and nonwoven fabrics. *J Appl Polym Sci* 2012; 125: 2271-2280.

33. Karthikeyan K, Russell B, Fleck N, et al. The effect of shear strength on the ballistic response of laminated composite plates. *European Journal of Mechanics-A/Solids* 2013; 42: 35-53.

34. Standard N. I. J. 0101.06. Ballistic Resistance of Body Armor 2008.

35. Dong Z and Sun CT. Testing and modeling of yarn pull-out in plain woven Kevlar fabrics. *Composites Part A: Applied Science and Manufacturing* 2009; 40: 1863-1869.

36. Cunniff PM. An analysis of the system effects in woven fabrics under ballistic impact. *Text Res J* 1992; 62: 495-509.

37. Chocron S, Ranjan Samant K, Nicholls AE, et al. Measurement of strain in fabrics under ballistic impact using embedded nichrome wires. Part I: Technique. *Int J Impact Eng* 2009; 36: 1296-1302.

38. Chocron S, Anderson Jr CE, Samant KR, et al. Measurement of strain in fabrics under ballistic impact using embedded nichrome wires, part II: Results and analysis. *Int J Impact Eng* 2010; 37: 69-81.

39. Chocron S, King N, Bigger R, et al. Impacts and Waves in Dyneema® HB80 Strips and Laminates. *Journal of Applied Mechanics* 2013; 80: 031806.

40. Tan VBC, Lim CT and Cheong CH. Perforation of high-strength fabric by projectiles of different geometry. *Int J Impact Eng* 2003; 28: 207-222.

41. Talebi H, Wong SV and Hamouda AMS. Finite element evaluation of projectile nose angle effects in ballistic perforation of high strength fabric. *Composite Structures* 2009; 87: 314-320.

42. Montgomery T, Grady P and Tomasino C. The effects of projectile geometry on the performance of ballistic fabrics. *Text Res J* 1982; 52: 442-450.

43. Lim C, Tan V and Cheong C. Perforation of high-strength double-ply fabric system by varying shaped projectiles. *Int J Impact Eng* 2002; 27: 577-591.

44. Prosser RA, Cohen SH and Segars RA. Heat as a factor in the penetration of cloth ballistic panels by 0.22 caliber projectiles. *Text Res J* 2000; 70: 709-722.

45. Tan V, Lim C and Cheong C. Perforation of high-strength fabric by projectiles of different geometry. *Int J Impact Eng* 2003; 28: 207-222.

46. Chen X, Zhu F and Wells G. An analytical model for ballistic impact on textile based body armour. *Composites Part B: Engineering* 2013; 45: 1508-1514.

47. Shim V, Guo Y and Tan V. Response of woven and laminated high-strength fabric to oblique impact. *Int J Impact Eng* 2012; 48: 87-97.

48. Shockey DA, Erlich DC and Simons JW. Lightweight fragment barriers for commercial aircraft. In: *Proceedings of the 18th International Symposium on Ballistics, San Antonio, TX, November 15-19, 1999; 1192-1199* .

49. Zeng XS, Shim VPW and Tan VBC. Influence of boundary conditions on the ballistic performance of high-strength fabric targets. *Int J Impact Eng* 2005; 32: 631-642.

50. Parsons EM, Weerasooriya T, Sarva S, et al. Impact of woven fabric: Experiments and mesostructure-based continuum-level simulations. *J Mech Phys Solids* 2010; 58: 1995-2021.

51. Shimek ME and Fahrenthold EP. Effects of Weave Type on Ballistic Performance of Fabrics. *AIAA J* 2012; 50: 2558-2565.

52. Kędzierski P, Popławski A, Gieleta R, et al. Experimental and Numerical Investigation of Fabric Impact Behavior. *Composites Part B: Engineering* 2014, 69: 452-459.

53. Lim JS, Lee BH, Lee CB, et al. Effect of the Weaving Density of Aramid Fabrics on Their Resistance to Ballistic Impacts. *Engineering* 2012; 4: 944.

54. Lim JS. Ballistic Behavior of Heracron®-Based Composites: Effect of the Number Multifilaments on High-Speed Projectiles. *Modeling and Numerical Simulation of Material Science* 2013; 3: 84.

55. Chen X, Zhou Y and Wells G. Numerical and experimental investigations into ballistic performance of hybrid fabric panels. *Composites Part B: Engineering* 2014; 58: 35-42.

56. Dong Z, Manimala JM and Sun C. Mechanical behavior of silica nanoparticle-impregnated Kevlar fabrics. *J Mech Mater Struct* 2010; 5: 529-548.

57. Shim VPW, Lim CT and Foo KJ. Dynamic mechanical properties of fabric armour. *Int J Impact Eng* 2001; 25: 1-15.

58. Zhu D, Mobasher B and Rajan SD. Dynamic tensile testing of Kevlar 49 fabrics. *J Mater Civ Eng* 2010; 23: 230-239.

59. Phoenix SL and Skelton J. Transverse Compressive Moduli and Yield Behavior of Some Orthotropic, High-Modulus Filaments. *Textile Research Journal* 1974; 44: 934-940.

60. Raftenburg MN, Scheidler NJ and Moy P. Transverse Compression Response of a Multi-Ply Kevlar Vest. Technical Report ARL-TR-3343. *Army Research Laboratory*. Aberdeen Proving Ground, MD, 2004.

61. Manimala JM and Sun C. Investigation of failure in Kevlar fabric under transverse indentation using a homogenized continuum constitutive model. *Text Res J* 2014; 84: 388-398.

62. Lomov SV, Willems A, Verpoest I, et al. Picture frame test of woven composite reinforcements with a full-field strain registration. *Text Res J* 2006; 76: 243-252.

63. Zhu D, Mobasher B, Vaidya A, et al. Mechanical behaviors of Kevlar 49 fabric subjected to uniaxial, biaxial tension and in-plane large shear deformation. *Composites Sci Technol* 2013; 74: 121-130.

64. Badel P, Vidal-Sallé E and Boisse P. Computational determination of in-plane shear mechanical behaviour of textile composite reinforcements. *Computational materials science* 2007; 40: 439-448.

65. Ha-Minh C, Imad A, Kanit T, et al. Numerical analysis of a ballistic impact on textile fabric. *Int J Mech Sci* 2013; 69: 32-39.

66. Song B and Lu W. Effect of twist on transverse impact response of ballistic fiber yarns. *Int J Impact Eng* 2015; 85: 1-4.

67. Bazhenov S, Dukhovskii I, Kovalev P, et al. The fracture of SVM aramide fibers upon a high-velocity transverse impact. *Polymer science.Series A, Chemistry, physics* 2001; 43: 61-71.

68. Carr D. Failure mechanisms of yarns subjected to ballistic impact. *J Mater Sci Lett 1999; 18: 585-588*.

69. Field JE and Sun Q. High-speed photographic study of impact on fibers and woven fabrics. In: *19th Intl Congress on High-Speed Photography and Photonics*, International Society for Optics and Photonics 1991; pp.703-712.

70. Heru Utomo B and Broos J. Dynamic material behavior determination using single fiber impact. In: *25th Conference and Exposition on Structural Dynamics, IMAC-XXV, Orlando, Florida, USA, February 19-22, 2007*.

71. Mulkern TJ and Raftenberg MN. Kevlar KM2 yarn and fabric strength under quasi-static tension Technical Report ARL-TR-2865. *Army Research Laboratory*. Aberdeen Proving Ground, MD, 2002.

72. Nilakantan G, Obaid AA, Keefe M, et al. Experimental evaluation and statistical characterization of the strength and strain energy density distribution of Kevlar KM2 yarns: exploring length-scale and weaving effects. *J Composite Mater* 2011; 45: 1749-1769.

73. Tan V, Zeng X and Shim V. Characterization and constitutive modeling of aramid fibers at high strain rates. *Int J Impact Eng* 2008; 35: 1303-1313.

74. Zhu D, Mobasher B, Erni J, et al. Strain rate and gage length effects on tensile behavior of Kevlar 49 single yarn. *Composites Part A: Applied Science and Manufacturing* 2012; 43: 2021-2029.

75. Dooraki BF, Nemes J and Bolduc M. Study of parameters affecting the strength of yarns. *Journal de Physique IV (Proceedings) 2006;* 1183-1188.

76. Languerand D, Zhang H, Murthy N, et al. Inelastic behavior and fracture of high modulus polymeric fiber bundles at high strain-rates. *Materials Science and Engineering: A* 2009; 500: 216-224.

77. Kirkwood KM, Kirkwood JE, Lee YS, et al. Yarn Pull-Out as a Mechanism for Dissipating Ballistic Impact Energy in Kevlar® KM-2 Fabric Part I: Quasi-Static Characterization of Yarn Pull-Out. *Text Res J* 2004; 74: 920-928.

78. Kirkwood JE, Kirkwood KM, Lee YS, et al. Yarn Pull-Out as a Mechanism for Dissipating Ballistic Impact Energy in Kevlar® KM-2 Fabric Part II: Predicting Ballistic Performance. *Text Res J* 2004; 74: 939-948.

79. Zhu D, Soranakom C, Mobasher B, et al. Experimental study and modeling of single yarn pull-out behavior of kevlar® 49 fabric. *Composites Part A: Applied Science and Manufacturing* 2011; 42: 868-879.

80. Bilisik K. Properties of yarn pull-out in para-aramid fabric structure and analysis by statistical model. *Composites Part A: Applied Science and Manufacturing* 2011; 42: 1930-1942.

81. Gawandi A, Thostenson ET and Gilllespie Jr JW. Tow pullout behavior of polymer-coated Kevlar fabric. *J Mater Sci* 2011; 46: 77-89.

82. Nilakantan G and Gillespie JW. Yarn pull-out behavior of plain woven Kevlar fabrics: Effect of yarn sizing, pullout rate, and fabric pre-tension. *Composite Structures* 2013; 101: 215-224.

83. Guo Z, Hong J, Zheng J, et al. Loading rate effects on dynamic out-of-plane yarn pull-out. *Text Res J* 2014; 84(16): 1708-1719.

84. Guo Z, Hong J, Zheng J, et al. Out-of-plane effects on dynamic pull-out of p-phenylene terephthalamide yarns. *Text Res J* 2014; 85(2), 140-149.

85. Rao Y and Farris RJ. A modeling and experimental study of the influence of twist on the mechanical properties of high-performance fiber yarns. *J Appl Polym Sci* 2000; 77: 1938-1949.

86. Chu Y, Chen X, Wang Q, et al. An Investigation on Sol-gel Treatment to Aramid Yarn to Increase Inter-yarn Friction. *Appl Surf Sci* 2014; 320: 710-717.

87. Cheng M, Chen W and Weerasooriya T. Experimental investigation of the transverse mechanical properties of a single Kevlar® KM2 fiber. *Int J Solids Structures* 2004; 41: 6215-6232.

88. Cheng M, Chen W and Weerasooriya T. Mechanical Properties of Kevlar® KM2 Single Fiber. Journal of Engineering Materials and Technology 2005; 127: 197-203.

89. Leal AA, Deitzel JM and Gillespie JW. Compressive strength analysis for high performance fibers with different modulus in tension and compression. *J Composite Mater* 2009; 43: 661-674.

90. Beckwith SW. Composites Reinforcement Fibers: II-The Aramid and Polyethylene Families. *SAMPE J* 2009; 45 (6), 42-43.

91. Kim J, Heckert N, McDonough W, et al. Statistical Characterization of Single PPTA Fiber Tensile Properties from High Strain Rate Tests. In: *Dynamic Behavior of Materials, Volume 1*, 2015, p.5-8.

92. Lim J, Chen WW and Zheng JQ. Dynamic small strain measurements of Kevlar® 129 single fibers with a miniaturized tension Kolsky bar. *Polym Test* 2010; 29: 701-705.

93. Lim J, Zheng J, Masters K, et al. Mechanical behavior of A265 single fibers. *Journal of Materials Science* 2010; 45: 652-661.

94. Hudspeth M, Claus B, Parab N, et al. In Situ Visual Observation of Fracture Processes in Several High-Performance Fibers. *Journal of Dynamic Behavior of Materials* 2015; 1(1): 55-64.

95. Kim JH, Alan Heckert N, Leigh SD, et al. Statistical analysis of PPTA fiber strengths measured under high strain rate condition. *Composites Sci Technol* 2014; 98: 93-99.

96. Lim J, Zheng JQ, Masters K, et al. Effects of gage length, loading rates, and damage on the strength of PPTA fibers. *Int J Impact Eng* 2011; 38: 219-227.

97. Schwartz P, Netravali A and Sembach S. Effects of strain rate and gauge length on the failure of ultra-high strength polyethylene fibers. *Text Res J* 1986; 56: 502-508.

98. Kawabata S. Measurement of the Transverse Mechanical Properties of High-performance Fibres. *Journal of The Textile Institute* 1990; 81: 432-447.

99. Singletary J, Davis H, Ramasubramanian MK, et al. The transverse compression of PPTA fibers Part I Single fiber transverse compression testing. *Journal of Materials Science* 2000; 35: 573-581.

100. Singletary J, Davis H, Song Y, et al. The transverse compression of PPTA fibers Part II Fiber transverse structure. *Journal of Materials Science* 2000; 35: 583-592.

101. Ruan F and Bao L. Mechanical enhancement of UHMWPE fibers by coating with carbon nanoparticles. *Fibers and Polymers* 2014; 15: 723-728.

102. Guo Z, Casem D, Hudspeth M, et al. Transverse compression of two high-performance ballistic fibers. *Text Res J* 2015; 1-10.

103. Wollbrett-Blitz J, Joannès S, Bruant R, et al. Multiaxial mechanical behavior of aramid fibers and identification of skin/core structure from single fiber transverse compression testing. Journal of *Polymer Science Part B: Polymer Physics* 2015; 54(3): 374-384.

104. Leal AA, Deitzel JM and Gillespie JW. Assessment of compressive properties of high performance organic fibers. *Composites Sci Technol* 2007; 67: 2786-2794.

105. M'Ewen E. XLI. Stresses in elastic cylinders in contact along a generatrix (including the effect of tangential friction). *Philosophical Magazine Series* 7 1949; 40: 454-459.

106. Hadley DW, Ward IM and Ward J. The Transverse Compression of Anisotropic Fibre Monofilaments. *Proceedings of the Royal Society of London Series A Mathematical and Physical Sciences* 1965; 285: 275-286.

107. Kotani T, Sweeney J and Ward IM. The measurement of transverse mechanical properties of polymer fibres. *Journal of Materials Science* 1994; 29: 5551-5558.

108. Pinnock PR, Ward IM and Wolfe JM. The Compression of Anisotropic Fibre Monofilaments. II. *Proceedings of the Royal Society of London Series A Mathematical and Physical Sciences* 1966; 291: 267-278.

109. Timoshenko S and Goodier JN. Theory of Elasticity, *McGraw-Hill*, 1951.

110. Obaid AA, Yarlagadda S and Gillespie Jr JW. Combined Effects of Kink Bands and Hygrothermal Conditioning on Tensile Strength of Polyarylate LCP and Aramid Fibers. *Journal of Composite Materials* 2015; 50(3): 339-350.

111. Kollár LP and Springer GS. Mechanics of composite structures, *Cambridge University Press*, 2003.

112. Tsai C and Daniel I. Determination of shear modulus of single fibers. *Exp Mech* 1999; 39: 284-286.

113. Sanborn BD and Weerasooriya T. Effect of Strain Rates and Pre-Twist on Tensile Strength of Kevlar KM2 Single Fiber. Technical Report ARL-TR-6403 *Army Research Laboratory*. Aberdeen Proving Ground, MD, 2013.

114. Sanborn B and Weerasooriya T. Quantifying damage at multiple loading rates to Kevlar KM2 fibers due to weaving, finishing, and pre-twist. *Int J Impact Eng* 2014; 71: 50-59.

115. Hudspeth M, Nie X and Chen W. Dynamic failure of Dyneema SK76 single fibers under biaxial shear/tension. *Polymer* 2012; 53: 5568-5574.

116. Hudspeth M, Li D, Spatola J, et al. The effects of off-axis transverse deflection loading on the failure strain of various high-performance fibers. *Text Res J* 2015; DOI: 10.1177/0040517515588262.

117. Hudspeth M, Chen W and Zheng J. Why the Smith theory over-predicts instant rupture velocities during fiber transverse impact. *Text Res J 2015*; DOI: 10.1177/0040517515586158.

118. Rao Y, Waddon AJ and Farris RJ. The evolution of structure and properties in poly(p-phenylene terephthalamide) fibers. *Polymer* 2001; 42: 5925-5935.

119. McAllister QP, Gillespie JW and VanLandingham MR. Evaluation of the three-dimensional properties of Kevlar across length scales. *Journal of Materials Research* 2012; 27: 1824-1837.

120. McAllister QP, Gillespie Jr JW and VanLandingham MR. The influence of surface microstructure on the scratch characteriztics of Kevlar fibers. *Journal of Materials Science* 2013; 48: 292-1302.

121. Li S, McGhie A and Tang S. Comparative study of the internal structures of Kevlar and spider silk by atomic force microscopy. *Journal of Vacuum Science & Technology A* 1994; 12: 1891-1894.

122. McAllister QP. The energy dissipative mechanisms of the particle-fiber interface in a textile composite, PhD Dissertation, University of Delaware, 2013.

123. Cole DP and Strawhecker KE. An improved instrumented indentation technique for single microfibers. *J Mater Res* 2014; 29: 1104-1112.

124. McAllister QP, Gillespie JW and VanLandingham MR. The energy dissipative mechanisms of particle-fiber interactions in a textile composite. *Journal of Composite Materials* 2013.

125. McAllister QP, Gillespie Jr JW and VanLandingham MR. The sub-micron scale energy dissipative deformation mechanisms of Kevlar fibrils. *Journal of Materials Science* 2013; 48: 6245-6261.

126. Decker M, Halbach C, Nam C, et al. Stab resistance of shear thickening fluid (STF)-treated fabrics. *Composites Sci Technol* 2007; 67: 565-578.

127. Tan V, Tay T and Teo W. Strengthening fabric armour with silica colloidal suspensions. *Int J Solids Structures* 2005; 42: 1561-1576.

128. LaBarre E, Calderon-Colon X, Morris M, et al. Effect of a carbon nanotube coating on friction and impact performance of Kevlar. *J Mater Sci* 2015; 50:5431-5442.

129. McDaniel PB, Deitzel JM and Gillespie JW. Structural Hierarchy and Surface Morphology of Highly Drawn Ultra High Molecular Weight Polyethylene Fibers Studied by Atomic Force Microscopy and Wide Angle X-Ray Diffraction. *Polymer* 2015; 69:148-158.

130. Pennings A. Bundle-like nucleation and longitudinal growth of fibrillar polymer crystals from flowing solutions. *Journal of Polymer Science: Polymer Symposia* 1977; 59: 55-86.

131. Strawhecker KE and Cole DP. Morphological and local mechanical surface characterization of ballistic fibers via AFM. *J Appl Polym Sci* 2014; 131(19).

132. Marissen R. Design with ultra strong polyethylene fibers. *Materials Sciences and Applications* 2011; 2: 319.

133. Ivanov I and Tabiei A. Loosely woven fabric model with viscoelastic crimped fibres for ballistic impact simulations. *Int J Numer Methods Eng* 2004; 61: 1565-1583.

134. King MJ, Jearanaisilawong P and Socrate S. A continuum constitutive model for the mechanical behavior of woven fabrics. *Int J Solids Structures* 2005; 42: 3867-3896.

135. Parsons EM, King MJ and Socrate S. Modeling yarn slip in woven fabric at the continuum level: Simulations of ballistic impact. *J Mech Phys Solids* 2013; 61: 265-292.

136. Shahkarami A and Vaziri R. A continuum shell finite element model for impact simulation of woven fabrics. *Int J Impact Eng* 2007; 34: 104-119.

137. Lim CT, Shim VPW and Ng YH. Finite-element modeling of the ballistic impact of fabric armor. *Int J Impact Eng* 2003; 28: 13-31.

138. Bansal S, Mobasher B, Rajan S, et al. Development of fabric constitutive behavior for use in modeling engine fan blade-out events. *J Aerospace Eng* 2009; 22: 249-259.

139. Stahlecker Z, Mobasher B, Rajan SD, et al. Development of reliable modeling methodologies for engine fan blade out containment analysis. Part II: Finite element analysis. *Int J Impact Eng* 2009; 36: 447-459.

140. Nadler B, Papadopoulos P and Steigmann DJ. Multiscale constitutive modeling and numerical simulation of fabric material. *Int J Solids Structures* 2006; 43: 206-221.

141. Boljen M and Hiermaier S. Continuum constitutive modeling of woven fabrics. *The European Physical Journal-Special Topics* 2012; 206: 149-161.

142. Grujicic M, Bell WC, Arakere G, et al. Development of a meso-scale material model for ballistic fabric and its use in flexible-armor protection systems. *Journal of Materials Engineering and Performance* 2010; 19: 22-39.

143. Erol O, Wetzel ED and Keefe M. Simulation of a textile sleeve on a manikin arm undergoing elbow flexion: effect of arm-sleeve friction. *The Journal of The Textile Institute* 2014; 106:10, 1135-1146.

144. Duan Y, Keefe M, Bogetti TA, et al. Modeling friction effects on the ballistic impact behavior of a single-ply high-strength fabric. *Int J Impact Eng* 2005; 31: 996-1012.

145. Nilakantan G, Keefe M, Bogetti TA, et al. On the finite element analysis of woven fabric impact using multiscale modeling techniques. *Int J Solids Structures* 2010; 47: 2300-2315.

146. Wang Y, Miao Y, Swenson D, et al. Digital element approach for simulating impact and penetration of textiles. *Int J Impact Eng* 2010; 37: 552-560.

147. Grujicic M, Hariharan A, Pandurangan B, et al. Fiber-level modeling of dynamic strength of Kevlar KM2 ballistic fabric. *Journal of Materials Engineering and Performance* 2012; 21: 1107-1119.

148. Nilakantan G. Filament-level modeling of Kevlar KM2 yarns for ballistic impact studies. *Composite Structures* 2013; 104: 1-13.

149. Hudspeth M, Agarwal A, Andrews B, et al. Degradation of yarns recovered from soft-armor targets subjected to multiple ballistic impacts. *Composites Part A: Applied Science and Manufacturing* 2014; 58: 98-106.

150. Freeston WD and Claus WD. Strain-wave reflections during ballistic impact of fabric panels. *Text Res J* 1973; 43: 348-351.

151. Roylance D. Wave propagation in a viscoelastic fiber subjected to transverse impact. *Journal of Applied Mechanics* 1973; 40: 143-148.

152. Cunniff P, Ting CTJ and Roylance D. Numerical Characterization of the Effects of Transverse Yarn Interaction on Textile Ballistic Response 1998; http://web.mit.edu/roylance/www/Ting_98.pdf.

153. Tan V and Ching T. Computational simulation of fabric armour subjected to ballistic impacts. *Int J Impact Eng* 2006; 32: 1737-1751.

154. Shim VPW, Tan VBC and Tay TE. Modelling deformation and damage characteristics of woven fabric under small projectile impact. *Int J Impact Eng* 1995; 16: 585-605.

155. Zeng X, Tan V and Shim V. Modelling inter-yarn friction in woven fabric armour. *Int J Numer Methods Eng* 2006; 66: 1309-1330.

156. Novotny WR, Cepuš E, Shahkarami A, et al. Numerical investigation of the ballistic efficiency of multi-ply fabric armours during the early stages of impact. *Int J Impact Eng* 2007; 34: 71-88.

157. Blankenhorn G, Schweizerhof K and Finckh H. Improved numerical investigations of a projectile impact on a textile structure. *Fourth European LS-DYNA Users Conference,* 2003.

158. Rao MP, Duan Y, Keefe M, et al. Modeling the effects of yarn material properties and friction on the ballistic impact of a plain-weave fabric. *Composite Structures* 2009; 89: 556-566.

159. Nilakantan G, Wetzel ED, Bogetti TA, et al. A deterministic finite element analysis of the effects of projectile characteristics on the impact response of fully clamped flexible woven fabrics. *Composite Structures* 2013; 95: 191-201.

160. Nilakantan G and Gillespie Jr. JW. Ballistic impact modeling of woven fabrics considering yarn strength, friction, projectile impact location, and fabric boundary condition effects. *Composite Structures* 2012; 94: 3624-3634.

161. Duan Y, Keefe M, Bogetti T, et al. A numerical investigation of the influence of friction on energy absorption by a high-strength fabric subjected to ballistic impact. *Int J Impact Eng* 2006; 32: 1299-1312.

162. Duan Y, Keefe M, Bogetti TA, et al. Modeling the role of friction during ballistic impact of a high-strength plain-weave fabric. *Composite Structures* 2005; 68: 331-337.

163. Barauskas R and Abraitienė A. Computational analysis of impact of a bullet against the multilayer fabrics in LS-DYNA. *Int J Impact Eng* 2007; 34: 1286-1305.

164. Rao MP, Nilakantan G, Keefe M, et al. Global/Local Modeling of Ballistic Impact onto Woven Fabrics. *Journal of Composite Materials* 2009; 43: 445-467.

165. Gogineni S, Gao X, David N, et al. Ballistic impact of Twaron CT709® plain weave fabrics. *Mechanics of Advanced Materials and Structures* 2012; 19: 441-452.

166. Gu B. Ballistic penetration of conically cylindrical steel projectile into plain-woven fabric target–a finite element simulation. *J Composite Mater* 2004; 38: 2049-2074.

167. Sun D, Chen X, Lewis E, et al. Finite element simulation of projectile perforation through a ballistic fabric. *Text Res J* 2012; 83(14): 1489-1499.

168. Jia X, Huang Z, Zu X, et al. Effect of Mesoscale and Multiscale Modeling on the Performance of Kevlar Woven Fabric Subjected to Ballistic Impact: A Numerical Study. *Applied Composite Materials* 2013; 20: 1195-1214.

169. Yen C, Scott B, Dehmer P, et al. A comparison between experiment and numerical simulation of fabric ballistic impact. In: *Proc. 23rd Int. Ballistic Symposium. Tarragona, Spain,* 2007.

170. Jiang Y, Tabiei A and Simitses GJ. A novel micromechanics-based approach to the derivation of constitutive equations for local/global analysis of a plain-weave fabric composite. *Composites Sci Technol* 2000; 60: 1825-1833.

171. Zohdi T and Powell D. Multiscale construction and large-scale simulation of structural fabric undergoing ballistic impact. *Comput Methods Appl Mech Eng* 2006; 195: 94-109.

172. Zohdi T. Microfibril-based estimates of the ballistic limit of multilayered fabric shielding. *Int J Fract* 2009; 158: 81-88.

173. Xia W, Adeeb SM and Nadler B. Ballistic performance study of fabric armor based on numerical simulations with multiscale material model. *Int J Numer Methods Eng* 2011; 87: 1007-1024.

174. Xia W and Nadler B. Three-scale modeling and numerical simulations of fabric materials. *Int J Eng Sci* 2011; 49: 229-239.

175. Nilakantan G, Keefe M, Wetzel ED, et al. Computational modeling of the probabilistic impact response of flexible fabrics. *Composite Structures* 2011; 93: 3163-3174.

176. Nilakantan G, Keefe M, Wetzel ED, et al. Effect of statistical yarn tensile strength on the probabilistic impact response of woven fabrics. *Composites Sci Technol* 2012; 72: 320-329.

177. Gasser A, Boisse P and Hanklar S. Mechanical behaviour of dry fabric reinforcements. 3D simulations versus biaxial tests. *Computational Materials Science* 2000; 17: 7-20.

178. Durville D. Finite element simulation of the mechanical behaviour of textile composites at the mesoscopic scale of individual fibers. In: *Textile Composites and Inflatable Structures II*, Springer Netherlands, 2008.

179. YUYANG M, AO J, AN YU Y, et al. Energy Loss Due to Transverse Plastic Deformation of Fibers in Textile Fabric Impact Processes. In: Liu, D., *Dynamic Effects in Composites* 2012; 103.

180. Sockalingam S, Gillespie Jr. JW and Keefe M. Modeling the transverse compression response of Kevlar KM2. In: *Proceedings of the American Society for Composites (ASC) 28th Technical Conference*, College Park, PA, USA. 2013.

181. Sockalingam S, Gillespie Jr. JW and Keefe M. On the transverse compression response of Kevlar KM2 using fiber-level finite element model. *International Journal of Solids and Structures* 2014; 51: 2504-2517.

182. Sockalingam S, Gillespie Jr. JW and Keefe M. Dynamic modeling of Kevlar KM2 single fiber subjected to transverse impact. *Int J Solids Structures* 2015; 67–68: 297-310.

183. Recchia S, Zheng JQ, Horner S, et al. Multiscale modeling of randomly interwoven fibers for prediction of KM2 Kevlar yarn strength and damage. *Acta Mech* 2015: 1-10.

184. Sockalingam S, Bremble R, Gillespie Jr. JW, et al. Transverse compression behavior of Kevlar KM2 single fiber. *Composites Part A: Applied Science and Manufacturing* 2016; 81: 271-281.

185. Allen MP and Tildesley DJ. Computer simulation of liquids, *Oxford University Press* 1987.

186. Chen C, Depa P, Maranas JK, et al. Comparison of explicit atom, united atom, and coarse-grained simulations of poly (methyl methacrylate). *J Chem Phys* 2008; 128: 124906-1-12.

187. Grujicic M, Bell W, Glomski P, et al. Filament-level modeling of aramid-based high-performance structural materials. *Journal of materials engineering and performance* 2011; 20: 1401-1413.

188. Grujicic M, Glomski P, Pandurangan B, et al. Multi-length scale computational derivation of Kevlar® yarn-level material model. *J Mater Sci* 2011; 46: 4787-4802.

189. Grujicic M, Yavari R, Ramaswami S, et al. Molecular-level study of the effect of prior axial compression/torsion on the axial-tensile strength of PPTA fibers. *Journal of materials engineering and performance* 2013; 22: 3269-3287.

190. Sun H. COMPASS: an ab initio force-field optimized for condensed-phase applications overview with details on alkane and benzene compounds. *The Journal of Physical Chemistry B* 1998; 102: 7338-7364.

191. Greenhalgh E, Bloodworth V, Iannucci L, et al. Fractographic observations on Dyneema® composites under ballistic impact. *Composites Part A: Applied Science and Manufacturing* 2013; 44: 51-62.

192. Chowdhury SC, Sockalingam S and Gillespie Jr JW. Molecular dynamics modeling of compression kinking in Kevlar. In: *SAMPE Conference Proceedings*, Baltimore, MD, USA, May 18-21, 2015.

193. Mayo J and Wetzel E. Cut resistance and failure of high-performance single fibers. *Text Res J* 2014; 84(12): 1233-1246.

194. Thomas JA, Shanaman MT, Lomicka CL, et al. Multiscale modeling of high-strength fibers and fabrics. In: *SPIE Defense, Security, and Sensing*, International Society for Optics and Photonics, 2012.

195. Lomicka C, Thomas J, LaBarre E, et al. Improving Ballistic Fiber Strength: Insights from Experiment and Simulation. In: Song, B., Casem, D., Kimberley, J., *Dynamic Behavior of Materials, Volume 1*, 2014, p.187-193.

196. Recchia SS, Pelegri A, Clawson JK, et al. A hierarchical model for Kevlar fiber failure. In: *ASME 2013 International Mechanical Engineering Congress and Exposition*, American Society of Mechanical Engineers. 2013.

197. Chowdhury SC, Staniszewski J, Martz EM, et al. A computational approach for linking molecular dynamics to finite element simulation of polyethylene fibers. In: *American Society of Composites - 30th Technical Conference*, East Lansing, MI, USA, September 28-30, 2015.

198. Boyd RH, Gee RH, Han J, et al. Conformational dynamics in bulk polyethylene: A molecular dynamics simulation study. *J Chem Phys* 1994; 101: 788-797.

199. Brown D and Clarke JH. Molecular dynamics simulation of an amorphous polymer under tension. 1. Phenomenology. *Macromolecules* 1991; 24: 2075-2082.

200. Rottler J and Robbins MO. Growth, microstructure, and failure of crazes in glassy polymers. *Physical Review E* 2003; 68: 011801.

201. Yamamoto T. Molecular dynamics in fiber formation of polyethylene and large deformation of the fiber. *Polymer* 2013; 54: 3086-3097.

202. Curgul S, Van Vliet KJ and Rutledge GC. Molecular dynamics simulation of size-dependent structural and thermal properties of polymer nanofibers. *Macromolecules* 2007; 40: 8483-8489.

203. Hossain D, Tschopp M, Ward D, et al. Molecular dynamics simulations of deformation mechanisms of amorphous polyethylene. *Polymer* 2010; 51: 6071-6083.

204. Mattsson TR, Lane JMD, Cochrane KR, et al. First-principles and classical molecular dynamics simulation of shocked polymers. *Physical Review B* 2010; 81: 054103.

205. Chantawansri TL, Sirk TW, Byrd EF, et al. Shock Hugoniot calculations of polymers using quantum mechanics and molecular dynamics. *J Chem Phys* 2012; 137: 204901.

206. Silling SA. Reformulation of elasticity theory for discontinuities and long-range forces. *J Mech Phys Solids* 2000; 48: 175-209.

207. Xu J, Askari A, Weckner O, et al. Peridynamic analysis of impact damage in composite laminates. *J Aerospace Eng* 2008; 21: 187-194.